Comptes Rendus

Géoscience

Sciences de la Planète

Yves-Michel Le Nindre, Roger Brett Davies, Benoit Issautier, Leopold Krystyn, Denis Vaslet, Bruno Vrielynck and Abdullah Memesh

The Middle to Late Triassic of Central Saudi Arabia with emphasis on the Jilh Formation. Part II: sequence stratigraphy, depositional and structural history, correlations and paleogeography

Research article

Tribute to Jean Dercourt

The Middle to Late Triassic of Central Saudi Arabia with emphasis on the Jilh Formation. Part II: sequence stratigraphy, depositional and structural history, correlations and paleogeography

Yves-Michel Le Nindre [*, a]**, Roger Brett Davies** [b]**, Benoit Issautier** [c]**, Leopold Krystyn** [d]**,
Denis Vaslet** [e]**, Bruno Vrielynck** [f] **and Abdullah Memesh** [g]

[a] Geo-consultant (BRGM retired), 58 Rue Gustave Flaubert 45100, Orléans, France

[b] Davies Geoconsulting (retired), Wintergreen House, Queen's Road, Harrogate, North Yorkshire, HG2 0HB, UK

[c] BRGM, 3, Avenue Claude Guillemin, B.P. 36009, 45060, Orléans Cedex 2, France

[d] Dept. of Palaeontology (Geozentrum), University of Vienna, Althanstrasse 14, Josef-Holaubek-Platz 2 (UZA II) 1090 Vienna (retired), Austria

[e] Geo-consultant (BRGM retired), 275 Route Royale, 33240 La Lande de Pomerol, France

[f] Institut des Sciences de la Terre de Paris (UMR 7193), Université Pierre et Marie Curie (UPMC) (retired), France

[g] Saudi Geological Survey, 54141, Ahmed bin Mohammed Al Ashab St., Jeddah 21514, Saudi Arabia

E-mails: yc.lenindre@wanadoo.fr (Y.-M. Le Nindre),
davies.geoconsulting@btinternet.com (R. B. Davies), b.issautier@brgm.fr
(B. Issautier), leopold.krystyn@univie.ac.at (L. Krystyn), d-d.vaslet@wanadoo.fr
(D. Vaslet), bruno.vrielynck@orange.fr, bjm.vrielynck@orange.fr (B. Vrielynck),
Memesh.AM@sgs.gov.sa (A. Memesh)

Abstract. New biostratigraphic data reported by Le Nindre et al. (2023 – this volume) improve the sequence stratigraphic understanding of the Middle–Late Triassic mixed carbonate-silicilclastic Jilh Formation and overlying siliciclastic Minjur Formation at outcrop in Central Saudi Arabia. The Anisian Tr40, Ladinian Tr50, Julian Tr60, Tuvalian Tr70 and Alaunian Tr80 MFS are all identified and their ages discussed. A major Carnian–Norian hiatus (Tr80 SB) approximates to but notably cuts across the mapped Jilh–Minjur Formation boundary. A younger Late Norian–Rhaetian transgression (Tr90 MFS?) is also identified. All of these major transgressive–regressive sequences and hiatuses can be identified with confidence and correlated at the regional scale with time-equivalent carbonates. The ages of subsurface lithostratigraphic units identified elsewhere across the Arabian Plate, notably the "Jilh, Sefidar and Marker Dolomites", "Jilh Evaporite" (sometimes "Carnian Salinity Crisis") and the *incertae sedis* Baluti Formation, and their equivalence in the Saudi Arabian outcrops, are assessed in the light

* Corresponding author.

of these results. The presence of significant siliciclastics at the base of the Carnian stratigraphy ("Julian Clastic Event") is also discussed.

Ladinian conodont faunas belonging to the Sephardic Province (Iberia, North Africa) and associated vertebrate faunas confirm transgression from the north. Similar conclusions are drawn for the Carnian and Norian transgressions.

The improved geochronologic understanding enabled a reconstruction of the structural phases of the Jilh geohistory in four steps from Anisian to Norian, showing the relationships of retrogradation–progradation processes and tectonic pulses to hiatuses and periods of erosion. A synthetic sequence stratigraphy is proposed.

1. Introduction

This study is the second part of an updated reconstruction of the sedimentary complex formed by the Jilh Formation and the overlying Minjur Sandstone (Middle and Late Triassic) in Saudi Arabia and adjacent countries, principally, but not exclusively, from outcrop data. It builds on a factual litho- and biostratigraphic base set up in Part I [Le Nindre et al., 2023], which the reader should refer to, in a first stage.

Part I of this study (this volume), provided updated and detailed descriptions of the litho- and biostratigraphy of the Middle to Late Triassic Jilh Formation and Minjur Sandstone along a 50 km-wide outcrop belt extending between latitudes 28° N and 21° N, along the eastern margin of the Arabian Shield (Figure 1). Together with the Permian–Early Triassic Khuff Formation and the Early Triassic Sudair Shale, these formations form an unconformable cover over the Pre-Permian rocks, and are in turn unconformably overlain by Jurassic and younger formations [Powers et al., 1966, Powers, 1968]. Le Nindre et al. [1987, 1990b] published a revised description of the lithostratigraphy, biostratigraphy and sedimentology of the Permian–Triassic at outcrop, based on the results of the cover rock geological mapping program at 1:250,000 scale by the Directorate Mineral Resources of Saudi Arabia (DMMR) and France's Geological Survey (BRGM). More recent publications provide a detailed description and interpretation of the underlying Khuff Formation [e.g. Vachard et al., 2005, Vaslet et al., 2005] and overlying Minjur Sandstone [Issautier et al., 2012a,b, 2019, Figure 2].

Key results of Part I were provided by new analyses of conodonts, and a revision of previous ammonoids identifications, including a new specimen collected in 2016. In particular Part I identified an Early Norian hiatus of more than 10 Ma within the upper Jilh Formation accompanied by marine and fluvial erosion.

Most of the Arabian Plate suffers from poor biostratigraphic age control during the Triassic. It is only in a few sections near the margins of the Arabian Plate or outcrops such as those described in Part I that have yielded good faunal or floral evidence. This emphasises the importance of new biostratigraphic data from the Central Saudi Arabian outcrops (documented in Part I, this volume) to understanding the more regional picture.

This Part II describes the internal organization of the transgressive–regressive (T–R) depositional sequences in the Jilh Formation and Minjur Sandstone based on precise dating by conodonts and ammonoids. Comparisons are made to regional maximum flooding events. From this point, reference to stages and substages, palynozones, sequences and maximum floodings is preferred to lithological units. Building on this, it is possible to reconstruct the tectonic and depositional history of the Jilh Formation and provide an overall sequence stratigraphic framework for the Middle to Late Triassic outcrops. Applying this knowledge to published sections of the Jilh Formation in the Central Ghawar area and eastwards into the eastern Rub al Khali Bains [Deville de Periere et al., 2022] demonstrates the applicability of the scheme at a regional scale. By including new data on Minjur Sandstone stratigraphy [Issautier et al., 2019], this analysis provides a correlation tool for the entire Middle to Late Triassic stratigraphy, extending from the outcrops to subsurface sections at the platform scale regardless of lateral facies changes.

Biogeographic and paleogeographic considerations demonstrate the northerly provenance of transgressions in the Middle to Late Triassic setting. An updated chronostratigraphic chart of the Permian to Mid Toarcian sedimentation includes these new results and summarizes the overall time evolution of
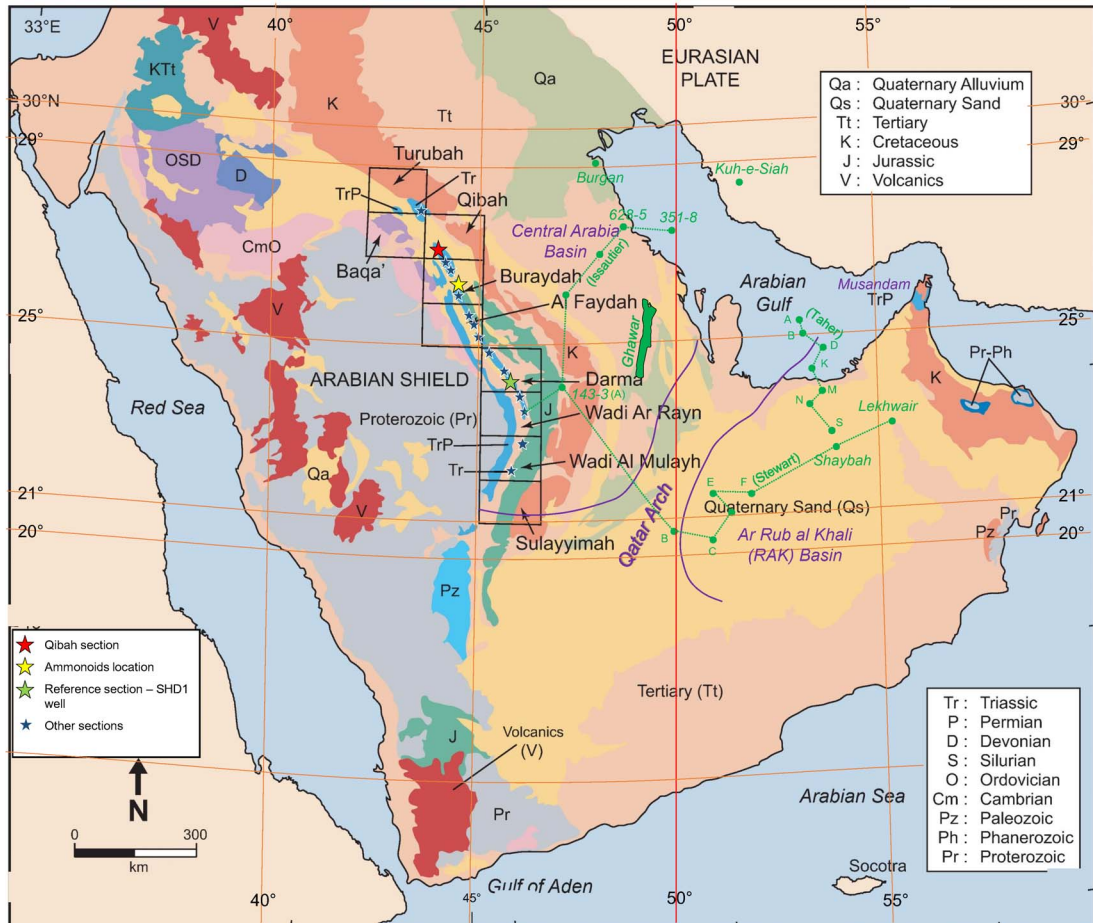
Figure 1. Simplified geological map of the Arabian Peninsula showing the quadrangles in which the Jilh Formation crops out. These quadrangles in Central Saudi Arabia were mapped by the DMMR (now Saudi Geological Survey) and France's BRGM (Hawasina nappes in Oman not shown, Qatar Arch from Stewart et al., 2016; in green, wells and transects cited in the text).

the depositional systems.

2. Geometry and ages of the depositional sequences

Accounting for both the system tracts geometry, obtained by mapping lithology and paleoenvironments, and the ages of the main marine intervals obtained from conodont and ammonite biostratigraphy in Part I, it is now possible to combine the two in order to reconstruct isochronous depositional sequences (Figure 5). This exercise demonstrates the importance of combining age and sequence stratigraphy to reconstruct a correct and

reliable geometry, based on genetic criteria. It faithfully reflects the depositional mechanisms, beyond the apparent lithostratigraphy, as seen section after section over more than 880 km. The results highlight structural processes, erosional surfaces and unconformities, as discussed below (Figures 6a–d and 7).

2.1. *Maximum flooding intervals and surfaces*

There is limited consensus on sequence stratigraphic schemes for the Triassic of the Arabian Plate, mainly due to the sparsity of biostratigraphic control. The most widely cited scheme, Sharland et al.'s [2001] sequence stratigraphic model for the
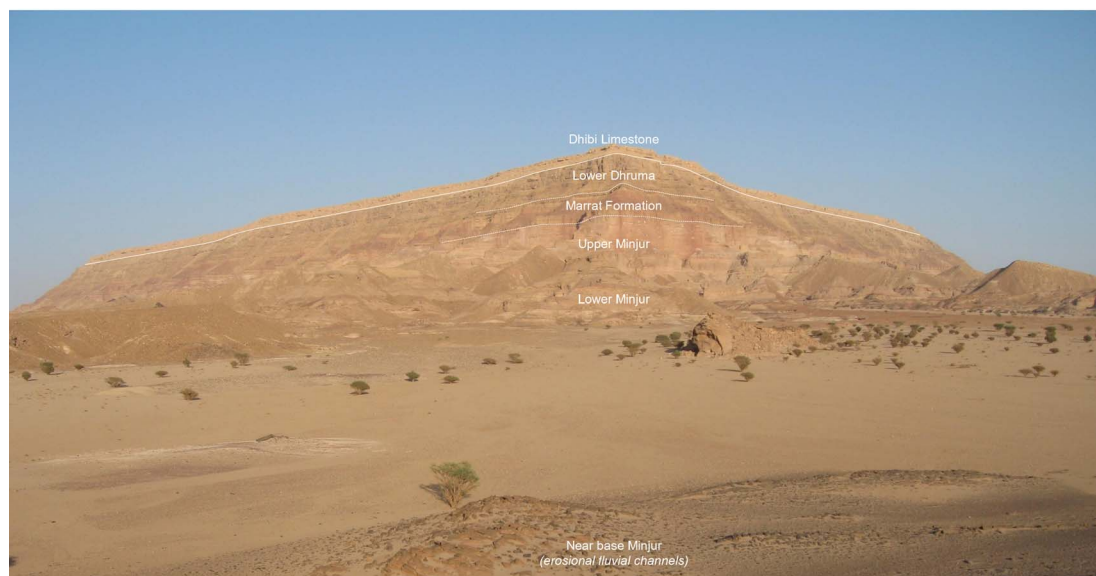
Figure 2. The Khashm al Khalta (K. al Minjur) promontory, type locality of the Minjur Sandstone, capped by the Marrat Formation, and the Lower Dhruma Formation; (c. 23°35′ N, 46°09′ E, Ar Rayn quadrangle). The foreground corresponds to the base of the Formation. The isolated hill of sandstone was interpreted as a flow tidal sand ridge [Sequence 2, Issautier et al., 2012a]. See Figure 3 for sequences and MFS interpretation in relation with the Jilh Formation. Photo Y. M. Le Nindre, Nov. 2008.

Middle to Late Triassic was based to a large degree on the succession in Iraq but subsequent publications demonstrate that it was misapplied over the southern half of the Arabian Plate including Saudi Arabia, particularly in their interpretation that the Anisian is missing. This led to a re-evaluation of Triassic sequence stratigraphy by a number of authors.

In this study, the maximum flooding surface nomenclature (MFS, Table 1) is adapted from Sharland et al. [2001, 2004] as revised by Davies and Simmons [2018], as their scheme has the best match with the new age data and stratigraphic organisation identified in the current study. Davies and Simmons [2018] proposed new reference sections for both MFS and SB on the Arabian Plate that had the best published biostratigraphic control. These tended to be in outcrops either towards the margins of the Arabian Plate, or along the Saudi Arabian outcrop where a fuller range of faunas and floras had been investigated and thus dating was better defined [e.g., Le Nindre et al., 1990b, 2023].

These MFS are positioned in our marine intervals (MFI) in outcrop (Figure 5) on the basis of the most commonly accepted ages of the surfaces, irrespective of the original sections taken for definition, which mostly suffer from poor or negligible biostratigraphic control (Table 1). The main marine surfaces/intervals containing fauna dated in Part I [Le Nindre et al., 2023] are MFS/MFI Tr40 (Anisian), Tr50 (Ladinian), Tr60 (Early Carnian), Tr70 (Late Carnian), and Tr80 (Norian). Then, the biostratigraphic ages of the surfaces have been refined according to the accuracy of the latest biostratigraphic results from outcrop. It is noteworthy that Deville de Periere et al. [2022], using palynology, also identify four sequences with comparable ages in the Jilh Formation of the eastern Rub al Khali Basin.

Numerical ages in the Triassic are poorly constrained with most stage boundaries only provisionally dated with few formal Global Boundary Stratotype Section and Points [GSSPs, nine for the Triassic in Ogg and Chen, 2020]. Thanks to the contribution of Moujahed Al-Husseini, we have tentatively assigned numerical ages to the successive MFS on the Arabian shelf by using the International Chronostratigraphic Chart v2015/01 [Cohen et al., 2013, updated; Ogg, 2012, 2015], and the software TimeScale Creator, version 6.4, February 2015. The age model for Version 6.4 is from "The Geologic Time Scale

Table 1. Tentative numerical ages (Ma) Triassic MFS on the Arabian shelf

Surface (this study)	Sharland et al. [2001] and GTS 96	Haq and Al-Qahtani [2005] and GTS 2004	Davies and Simmons [2018] GTS 2020	This study GTS 2020-03	Sequence [Ogg and Chen, 2020]	Sequence [Haq, 2018]	Age (Ma)	Max sea level (Ma)
Triassic/Jurassic				201.4			201.36	
Mid Norian MFS Tr80	215	211.0	Late Norian *c.* 213	217.0	TNo3?	TNo3?	222.5–217.3	?
Tuvalian MFS Tr70	222	220.0	Tuvalian *c.* 230	230.0	TCar2	TCa2	233.5–229.0	230
Latest Julian MFS Tr60	226	226.0	Julian *c.* 234.7	234.0	TCar1	TCa1	236.2–233.5	234.5
Late Ladinian MFS Tr50	233	234.0	E. Ladinian *c.* 241	239.0	TLad2	TLa2	239.5–238.0	238.5
Anisian MFS Tr40	238	241.0	Pelsonian *c.* 243.8	242.5	TAn3	TAn3	243.5–242.1	242.5
Olenekian MFS Tr30	245	249.8	Smithian *c.* 249	248.5	TIn3	TIn3	250.0–247.9	248.5

2012" [Gradstein et al., 2012], and the Triassic scale is by Ogg [2012].

The latest International Chronostratigraphic Chart 2022/10 [Cohen et al., 2013, updated] shows only very minor changes (on base Induan and top Rhaetian) from the 2015-01 version. Those changes do not materially affect our interpretations. The ages are the following: Base Induan: 251.9 Ma (252.17 in version 2015-01); Induan–Olenekian: 251.2; Olenekian–Anisian: 247.2; Anisian–Ladinian: 242; Ladinian–Carnian: 237; Carnian–Norian: 227; Norian–Rhaetian: 208.5; Rhaetian–Hettangian: 201.4 ± 0.2.

2.1.1. *Maximum flooding surface MFS Tr30 and MFS Tr40*

MFS Tr30. In this study we do not address the Early Triassic (mid-Scythian) MFS Tr30 of Sharland et al. [2001, 2004] but for the sake of completeness, we briefly mention it here. They picked MFS Tr30 within the upper Sudair Formation [Sharief, 1986], and dated it 245 Ma in GTS 1996. Haq and Al-Qahtani [2005] followed Sharland et al. by also picking MFS Tr30 in the Sudair Shale and revised its age to 249.75 Ma in the Olenekian (upper Scythian) in GTS 2004. More recently, Davies and Simmons [2018] have updated the plate-wide correlation of the Triassic T–R sequences in coordination with this study. In Saudi Arabia, MFS Tr30 was picked in the Sudair Shale in a bioclastic arenitic dolomite with marine

fauna at 187 m in the SHD-1 Well [Manivit et al., 1985a, Darmā quadrangle] and suggested to be of probable Early Olenekian (Smithian) age. The best candidate in the Haq [2018] and Ogg and Chen [2020] schemes would be in their sequence TIn3. Davies et al. [2019] identified strong diachroneity between siliciclastics of the Sudair and lower Jilh Formations and the carbonates and evaporites of the Dashtak Formation on opposite sides of the Arabian Gulf.

MFS Tr40. Sharland et al. [2001] interpreted Anisian MFS Tr40 in the Arabian Plate and dated it 238 Ma according to GTS 1996, but had not identified it in Saudi Arabia or neighbouring countries. Haq and Al-Qahtani [2005] revised the numerical age to 241 Ma in GTS 2004 and followed Sharland et al. in assuming it is missing due to a hiatus in the Anisian. While the Anisian age for MFS Tr40 remains valid, the numerical age assignments are clearly outmoded due to updates to the time scale. In Davies and Simmons [2018], a Mid-Anisian (Pelsonian) age of the MFS Tr40 is demonstrated by the presence of ammonoids of the Balatonicus zone in the Tethyan domain, and supported by the presence of the conodont *Nicoraella kockeli*, in carbonate beds of the Ra'af Formation (Negev southern Israel) taken as reference section.

Here we assign MFS Tr40 to the tidal and infralittoral bioclastic dolomite slab forming the first cuesta of the Jilh Formation at the outcrop from which the

SHD-1 Well was drilled. An equivalent horizon can be followed at the outcrop scale. This interpretation matches that of Davies and Simmons [2018] which was undertaken in concert with one of the authors (YML).

Given this biostratigraphic age, the MFS Tr40 best corresponds to sequence TAn2, from 244.24 (SB) to 243.33 Ma (TAn3 SB) and maximum sea level at 244 Ma in Haq [2018] and Ogg and Chen [2020], GSSP, adopted here.

2.1.2. *Maximum flooding surface MFS Tr50*

Sharland et al. [2001] dated MFS Tr50 at 233 Ma in the Ladinian and tentatively positioned it in the Jilh Formation in Saudi Arabia [Sharief, 1986, Vickers-Rich et al., 1999]. Haq and Al-Qahtani [2005] revised the numerical age to 234 Ma in GTS 2004, and picked it in the Ladinian part of the lower Jilh Formation. The Ladinian age remains valid but the numerical age has changed due to timescale updates. Davies and Simmons [2018] assigned it to "thin dolomite beds containing the conodont *Pseudofurnishius murcianus* immediately below the J1/J2 boundary in the Jilh Formation reference section at outcrop [Le Nindre et al., 1990b]".

In our study two marine episodes appear during the Ladinian, the first one characterised by *Budurovignathus truempyi*, and the second one by *B. mungoensis*. They both occur in the upper part of Unit J1. The first marine event is characterized by the association *P. shagami*, *P. murcianus* and *B. truempyi*. In one hypothesis, it thus would correspond to the mid–late Fassanian transgressive cycle TLad1 of GSSP 2020 [Ogg and Chen, 2020].

However, we interpret that the major MFS is defined instead by the southward extent of the *P. murcianus–B. mungoensis*, association of Late Ladinian (Longobardian) age, as explained in Part I. In fact, *Budurovignathus* appears associated with flooding events, and is recovered from the dolomitic benches, representing more offshore (deeper?) settings, whereas *Pseudofurnishius* is associated with the clastic regressive phase above, or more proximal (shallower?) settings. This hypothesis is supported by the vertical distribution of the conodonts where the two are present, and by restriction of *Budurovignathus* to a more marine area (lat. 24°27′ N–26°21′ N).

In the chart of Haq [2018], this time interval corresponds to a transgressive cycle TLa2 from 239.5

(SB) to 238 Ma (TLa3 SB), spanning the Longobardicum and Neumayri ammonite zones—early–mid Longobardian—with the maximum sea level at 238.5 Ma. The same is recorded in Ogg and Chen [2020]. This major carbonate marine event is recognized and dated all along the outcrop from Khashm Dolqan (24°15′ N) northward.

2.1.3. *Maximum flooding surface MFS Tr60*

Sharland et al. [2001] picked MFS Tr60 in the Jilh Formation in Saudi Arabia [Sharief, 1986, Vickers-Rich et al., 1999] and dated it at 226 Ma in the Carnian. Haq and Al-Qahtani [2005] also estimated its age as 226 Ma, and similarly picked it in the Carnian part of the lower Jilh Formation. Referring to Haq [2018], it best corresponds to the sequence TCa1 from 236.2 (SB) to 233.5 Ma (TCa2 SB), with the maximum eustatic sea level at 234.5 Ma.

In our study, Late Triassic, latest Julian (Early Carnian) MFS Tr60 occurs in mapped Unit J2, or mapped Unit J3 respectively north and south of 25° N. It is the major maximum flooding interval (MFI) of the Jilh Formation, as shown by the more transgressive facies, while the major clastic influx at the base of this sequence occurred in early Julian. This transgressive event reached up to Jabal al Arid (23°31′ N) where the dolomite on top of the Unit J3 contains *Quadralella polygnathiformis* (Carnian) with the southernmost marker of Julian, *P. inclinata*, at Khabra Halwah (23°55′ N) just beneath the pre-Minjur unconformity.

Davies and Simmons [2018], placed Tr60 in dolomitic beds bearing *Quadralella polygnathiformis* on top of the Unit J3 of the Khashm Dolqan reference section. Although these beds correctly represent the MFI, in fact the key markers (*P. inclinata*—Julian—and *Q. polygnathiformis*—Carnian *s.l.*) were provided by the neighbouring section of Khabra Halwah (VD80-328, 329) as explained above, and not by the reference section.

The numerical age of the Julian/Tuvalian boundary is not adequately constrained in GTS 2015 and may be about 233.6 Ma [Ogg, 2015, Ogg and Chen, 2020]. Furin et al. [2006] reported a ^{206}Pb/^{238}U age of 230.91 Ma ± 0.33 Ma for zircons from an ash bed within the range of the conodont *Metapolygnathus nodosus* in the middle–upper Tuvalian. These age estimates imply latest Julian MFS Tr60 is no younger than 230.9 Ma and probably older than 233.5 Ma, or

about 8 Ma older than previous estimates. We attribute an approximate age of about 234.0 Ma for latest Julian MFS Tr60.

2.1.4. *Maximum flooding surface MFS Tr70*

Sharland et al. [2001] did not identify MFS Tr70 in Saudi Arabia. Based on undated outcrop data from Iraq they estimated its age as 222 Ma, while Haq and Al-Qahtani [2005] estimated its numerical age as 220 Ma, both in the Late Carnian, and showed it in the Carnian part of the upper Jilh Formation. Davies and Simmons [2018] had identified it, based of work by one of the authors (YML), interpreting its age as Late Carnian on the ammonoid "*Clydonites* sp.," identification of which was reinterpreted in Part I. They also noted the presence of the conodont *P. inclinata* in the reference section. In fact, *P. inclinata* was found on top of a neighbouring section (VD80-328, 329, Khabra Halwah), and is a fossil marker of the Julian.

In our study, Tuvalian (Late Carnian) is identified in Unit J3, principally north of 25° N. The development of marine carbonates in the north with Tropitids and conodonts identifies this flooding event. The presence of the conodont *Quadralella carpathica* points to the early to middle Tuvalian, while Tuvalian 1 up to Tuvalian 2/I is indicated by the Tropitid ammonoids. A common associate is *Q. polygnathiformis.*

With a Carnian–Norian boundary at 227 Ma (ICC 2020/03 and 2022/10) and the base of Tuvalian at 233.6 Ma, an age of 230.91 ± 0.33 Ma in middle–upper Tuvalian is correct. Thus, we estimate the numerical age of MFS Tr70 around 230 Ma. This MFS best corresponds to sequence TCar2 in Ogg and Chen [2020] from 233.6 Ma (SB) to 228 Ma (TCar3 SB), with a maximum sea level at 230 Ma.

2.1.5. *Maximum flooding surface MFS Tr80*

In the literature, definitions and assignations of MFS Tr80 are uncertain and multiple, principally due to lack of reliable biostratigraphic or numerical ages. Furthermore, the Norian period was characterised by the broad extent of continental areas and sedimentary hiatuses [Davies and Simmons, 2018, Maurer et al., 2008, 2015]. This situation engendered subsequent confusing and conflicting interpretations.

Sharland et al. [2001] assigned a Norian age to MFS Tr80 (215 Ma, i.e., mid Norian in the time scale

of 1996) but age diagnostic fossils were lacking at the time of writing (apart from potentially Norian pollens in Kuwait). They did not identify Tr80 in Saudi Arabia although the surface was tentatively picked in neighbouring Kuwait and Abu Dhabi. Sharland et al. proposed a reference section near the base of the Sarki Formation in Iraq, although they acknowledged the absence of biostratigraphic age control. If the age of the Lower Sarki Formation is Norian [Hanna, 2007, Lunn et al., 2019], Sharland et al.'s interpretation that the "Marker Dolomite" of Lunn et al. near the top of the Kurra Chine Formation, equivalent to the Sefidar Dolomite, near the top of the Dashtak Formation in Iran, also contains MFS Tr80 cannot be correct. The Baluti Formation separates the underlying "Marker Dolomite" from the overlying Sarki Formation [Lunn et al., 2019]. Palynological data confirms that at least part (but not necessarily all) of the Baluti Formation is Late Carnian [only composite samples were analysed—Lunn et al., 2019], thereby confirming that the "Marker Dolomite" is also of Carnian age. The Sefidar Dolomite corresponds, by the underlying lithologic succession (dolomite–evaporite–dolomite) and by its wire line characteristic response to the "Marker Dolomite", elsewhere named "Jilh Dolomite" in Saudi Arabia. This equivalence is best demonstrated by the presence of the distinctive Jilh Dolomite in offshore gas fields, notably Karan, that lie adjacent to the median line with Iran [Sodagar, 2015]. This unit is assigned herein to the Early Carnian MFS Tr60 [see further paragraph 4.2 on "Jilh Dolomite" and Davies and Simmons, 2018].

As noted previously, Sharland et al. [2004] placed the MFS Tr80 in the early Middle Norian: from this point of view, it would correspond to our Alaunian 1 transgression dated in Part I. Haq and Al-Qahtani [2005, see their Enclosure 2] estimated its age as 211 Ma, and showed it in the Norian Minjur Formation.

Davies and Simmons [2018], revising Sharland et al. [2001], selected a new reference location for the MFS Tr80, in Musandam UAE. They picked the MFS within the Milaha Formation in the first limestone beds with megalodonts and crinoids, above the marker foraminifer *Triasina hantkeni* of late Middle Norian to Rhaetian age [Leopold Krystyn, Urban et al., 2023], and below the latest Norian beds of the Asfal Member (lower part of the Ghalilah Formation) dated by the ammonoid *Neotibetites* and by

the conodont *Epigondolella bidentata* [Maurer et al., 2008, 2015, location on Figure 1].

In accord with the present study, the sequence boundary (Tr80 SB) was picked in the Early Norian hiatus.

Additional graphical evidence presented by Urban et al. [2023] reveals that the boundary of the Milaha Formation and the overlying Asfal Member of the Ghalilah Formation is an erosional discontinuity marked by a reworked limestone conglomerate. This erosional discontinuity is an obvious candidate for an additional sequence boundary, which might be designated as Tr90 SB.

Issautier et al. [2019] have demonstrated that there are three maximum flooding intervals (MFI) in the Minjur Sandstone through a southwest–northeast transect from outcrop to the Gulf (location on Figure 1):

- **Early to Middle Norian**: in subsurface, beds containing the marine dinocyst *Rhaetogonyaulax wigginsii*. In Well 143-3, the closest to the outcrop (location on Figure 1), a thick sandstone interval was deposited between 1050 ft and 1150 ft (320–350 m), capped by a 50 ft (15 m) thick mudstone interval in which *R. wigginsii* was found at 1042 ft (318 m) (FDO and LDO). The palynology study revealed that this shallow marine bio-marker is the most widespread and could date the peak transgression within the Triassic portion of the Minjur Formation. The FDO of *R. wigginsii*, within the palynosubzone T1B, suggests a position close to the middle–early Norian boundary, following the work of Nicoll and Foster [1994, 1998] who correlated conodont zones with the ranges of selected dinoflagellate cysts, including *R. wigginsii*. In outcrop these beds are correlated with Minjur Sequence 4 [Issautier et al., 2012a, 2019] which is characterized, by a basal braided sand sheet overlain by cross-bedded sandstones representing tidal channels, bioturbated sandstones, and dolomitic siltstones representing associated mudflats.
- **Latest Norian–Early Rhaetian**: in subsurface locations, beds containing the dinocyst *Rhaetogonyaulax rhaetica*. In the SW–NE traverse studied by Issautier et al. [2019],

R. rhaetica occurrence is restricted to coastal well 628-5. In outcrop, Issautier et al. formulated three hypotheses: either the *R. rhaetica* transgression never reached the outcrop or was eroded by the intra-Minjur unconformity, or the *R. rhaetica* transgression might be partly equivalent to the transgressive systems tract of upper Sequence 5, represented by tidal flat and channel facies. Issautier et al. [2019] also correlated these beds with the Malihah and the lower Ghalilah formations (Asfal Member) of comparable age in the UAE section [Maurer et al., 2008, 2015].

- **Latest Rhaetian to Early Pliensbachian**: in subsurface, beds containing the dinocysts *Dapcodinium priscus,* for which no MFS *sensu* Sharland et al. [2001] has been identified. In outcrop, they are likely coeval with the transgressive intervals of the Minjur Sequences 6, 7, and 8 including marginal marine or tidal deposits. The upper one is underlined by marine carbonate in the upper part of the formation and would correspond to the uppermost tidal channel of Sequence 8. It seems probable that the as yet unidentified MFS is located in the overlying Early Jurassic (Hettangian–Sinemurian?) section. A comparable Rhaetian to Early Jurassic transgression can be identified in Kuwait [Kadar et al., 2015].

Issautier et al. [2012a, 2019] explain the different extents of the *R. wigginsii* and *R. rhaetica* transgressions by modified paleogeographic settings. A flatter landscape with tidal flats during Early–Mid Norian enabled retrogradation of *R. wigginsii* marine facies to more proximal settings. A more contrasted landscape during Late Norian and Rhaetian, with an upstream part supplying abundant clastics deterred landward retrogradation of *R. rhaetica* facies.

Fine-grained fluvial-lagoonal and littoral deposits containing echinoderms debris, were used for subdividing a lower from an upper unit in the Minjur Sandstone within the Ar Rayn quadrangle by Vaslet et al. [1983], and within the Al Mulayh quadrangle by Manivit et al. [1985b]. Due to lack of biostratigraphic constraints, it is not clear with which of the two Norian MFS's it is associated. However, the EarthVision® 3D model (by B. Issautier and Y.

M. Le Nindre, 2011, unpublished) shows a strict correspondence between Sequence 4 and the 90–130 m marker of the Khashm al Khalta section of Vaslet et al. [1983], which is taken as the base of the "Upper Unit' (Figure 3a). The ophiurid vertebrae were observed from the uppermost dolomitic siltstone beds (sample VD80-122, Figure 4).

The base of Sequence 4 truncates Sequence 3 and partially Sequence 2 of the Minjur Sandstone as a north-dipping surface observed in the field and modelled (EathVision® 3D, Figure 3b) by B. Issautier and Y. M. Le Nindre in 2011 [annex work to Issautier, 2011].

Issautier et al. [2019] thus assigned the MFS Tr80 to the early Middle Norian *R. wigginsii* beds, widespread on both sides of the Qatar Arch as shown by their figure 16 after Stewart et al. [2016]. It matches the Alaunian 1 ages obtained in Part I of our study, on top of the Jilh Formation and at the base of the Minjur Sandstone northwards of 25°30′ N, from ammonoids and from the conodonts *Ancyrogondolella praeslovakensis*, and *Epigondolella abneptis* in several sections.

Within this given context, for matter of simplification, and following Issautier et al. [2019], in the next pages we keep using Tr80 for the Alaunian 1 regional transgression separated from the Tuvalian Tr70 by a disconformity of more than 10 Ma. The renaming of Tr80 is out of the scope of this study. Nevertheless Tr80, Tr90, and either Tr100 or more likely J05, could be proposed for Alaunian (T1B), Sevatian (T1A), and latest Rhaetian–Early Pliensbachian (T0-J) transgressions, respectively. J10 is still in the overlying Marrat Formation.

The Emirates-Musandam section [Maurer et al., 2008, 2015, Urban et al., 2023] contains two transgressive events separated by an erosional discontinuity, the lower one at the base of the Milaha Formation, the upper one at the base of the Asfal member of the Ghalilah Formation. The only marker fossil recorded in the Milaha Formation is the foraminifer *Triasina hantkeni* which was recovered 21 m above its base and 50 m below the contact with the overlying Asfal Member [Maurer et al., 2008, 2015, Urban et al., 2023]. Davies and Simmons [2018] followed other workers in interpreting that the range of *T. hantkeni* was Late Norian (Sevatian) to Rhaetian, which accounts for their assignment of the MFS in the Milaha Formation to the Late Norian. However Urban

et al. argue that a Middle Norian age for *T. hantkeni* cannot be ruled out. This remains the opinion of one of the authors (LK) We note that *T. hantkeni* is commonly reported in lagoonal sediments also containing megalodonts, as is the case of the Milaha Formation, and therefore wonder if it may have been, at least partially, facies controlled. Consequently, the lower transgressive event could be (partly) contemporaneous of the Alaunian transgression in central Arabia, and the erosional surface capped by a conglomerate that separates the Milaha and Ghalilah Formations likely represents the same event that marks the base of Sequence 5 (scour surface SB5) of Issautier et al. [2019]. It would set up the interesting possibility that the upper transgression in the Asfal Member is (partly) equivalent to the *R. rhaetica* flooding as suggested by Issautier et al. [2019]. This would be consistent with the nomenclature suggested above, namely that the Alaunian transgression was associated with MFS Tr80, and that the younger Late Norian–Rhaetian event could represent a newly identified MFS Tr90.

Note that Lunn et al. [2019] and Lunn [2020] use "Tr80" (previously "Tr80 v1") in place of MFS Tr60 within the Jilh Dolomite unit (see Section 4: "Particular events and their regional correlations"). Lunn assigned a "Tr 100" (previously "Tr80 v3") to the *R. rhaetica* MFS in Wells 143-3 and 628-5, T1A palynosubzone, referring to Issautier et al. [2019]. Readers should note that Lunn misidentified the Jilh Dolomite equivalent in well 143-3.

In our study MFS Tr80 is interpreted as early Middle Norian and the base of the Alaunian is at 217.49 Ma [Ogg and Chen, 2020]. It could therefore correlate to MFS Nor1 in Time Scale Creator at c. 217 Ma, the best guess for the age of Tr80 so far (Table 1). However, in the Haq [2018] chart, as well as in the Ogg and Chen chart, this age corresponds to a sea level lowstand; subsequently, this transgression could eventually match the top of the TNo3 sequence in the Late Lacian, revealing that broad uncertainties exist on the Norian sea-level and coastal onlap curves.

In conclusion, at the regional scale (Iran, Iraq, Kuwait, UAE, Oman, Saudi Arabia), we have not yet in hand all the elements for establishing a hierarchy of the major flooding events of the Late Triassic at plate scale. Disagreements between the authors in a broader spectrum of papers on ages and correla-
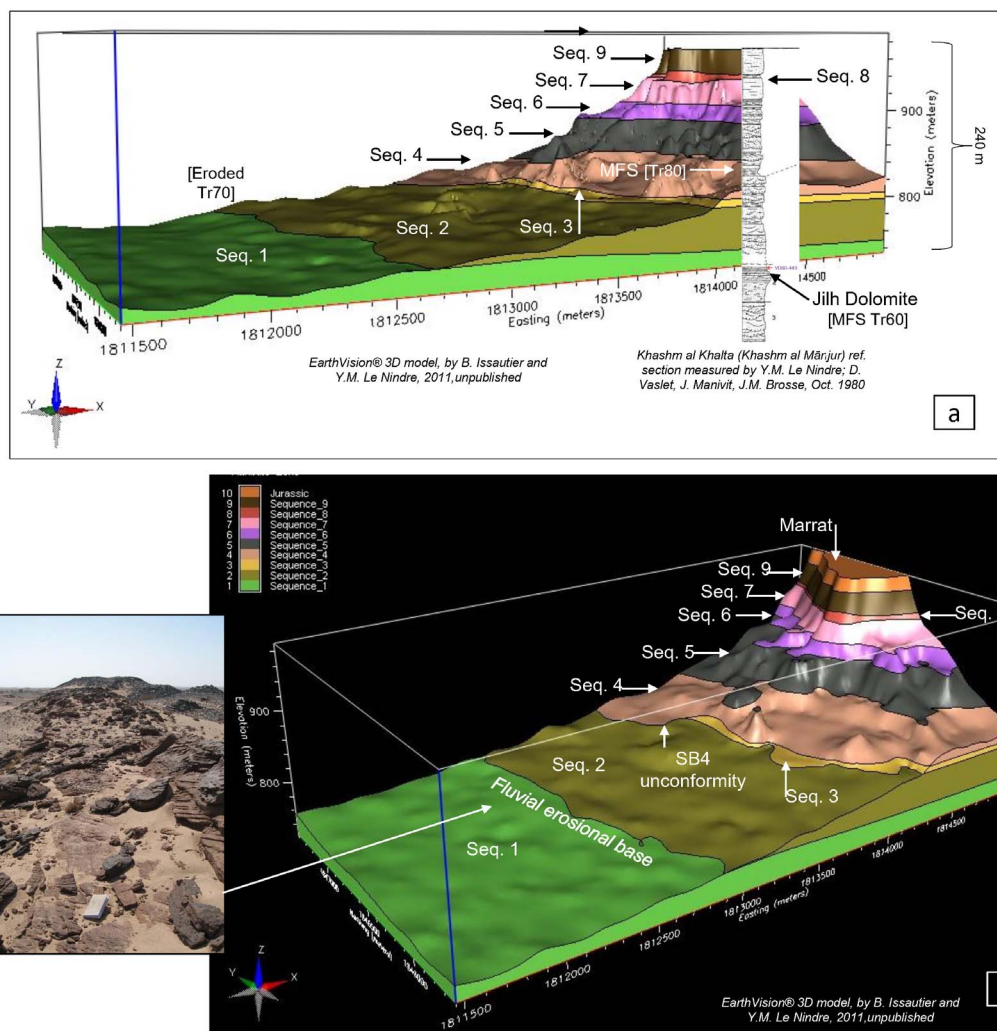
Figure 3. Learning from the Minjur 3D model at Khashm Al Khalta (Khasm al Mānjur) type locality. (a) Correspondence between the model and the section measured by Le Nindre and others in Oct. 1980—see Part I, Le Nindre et al. [2023]—with indication of the MFS [Tr80] horizon, and Jilh Dolomite Tr60. Tr70 is eroded from the North at this latitude—view from South; (b) Other view—from west-southwest—emphasizing the SB4 unconformity (early–mid Norian) and the pre-Minjur fluvial erosion (Carnian–Norian boundary). Minjur sequences nomenclature of Issautier et al. [2012a].

tions within this period persist due to an obvious lack in biostratigraphic data and in numerical ages for making reliable correlations regardless of the lithologies as we present now for Saudi Arabia. In particular outcrop paleontological studies using both ammonoids and conodonts are not developed sufficiently to confirm correlations in the subsurface using only well logs or facies associations and need further investigation.

2.2. *Depositional and structural evolution from Ladinian to Norian*

Using the available time markers (datums or assumed), we have split the geohistory of the Jilh Formation into four stages (Figures 6a to 9d). This exercise demonstrates the evolution of the structural setting, and the vertical and horizontal relationships between the successive depositional units.
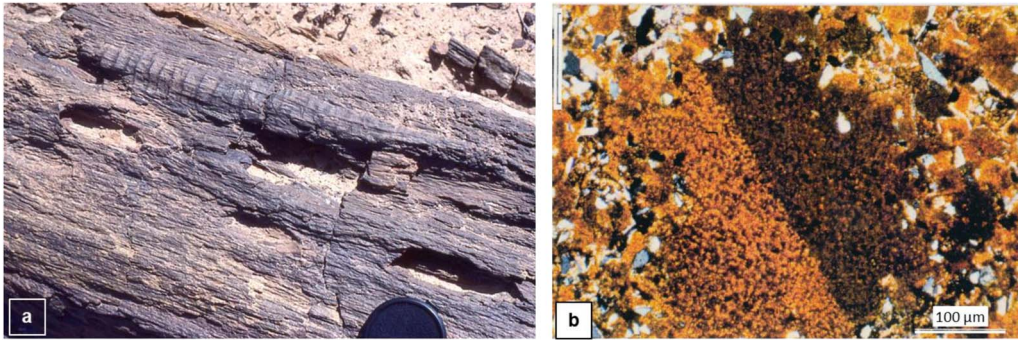
Figure 4. Two remarkable fossils of the Minjur Sandstone: silicified tree trunk (a), and skeletal piece of Ophiuridea (b). (a) Tree trunk (length ≤ 5 m, diameter ≤ 50 cm) of a Mid Norian petrified forest near Al Barud (c. 24°50′ N, 44°11′ E) Sample JMA83-238, Buraydah quadrangle. Photo J. Manivit. (b) Siltstone with angular and splinter quartz, cemented by dolomicrosparite, detail: typical section of ophiuroid vertebra reflecting temporary marine incursion into a dominantly fluvio-deltaic setting (MFS Tr80?). sample VD80-122, B28450, polarized light, Khashm al Khalta section (c. 23°35′ N, 46°10′ N), Ar Rayn quadrangle. Photo Y. M. Le Nindre.

In Figure 6, we have intentionally abandoned the use of the lithological units J1 to J3 since Part I established diachroneity in these units. Instead, we introduce letters A to J to denote "horizons"; i.e., layers with relatively uniform facies and thicknesses. Several horizons contain individual "bodies" that represent lateral changes in facies or thickness, such as those that represent the Julian Clastic Event. The numbers 1 to 11 are "surfaces", time lines or events (e.g., MFS, SB) and they separate horizons that can be interpreted as subaerial sequence boundary (SB), transgressive (TST) and highstand (HST) systems tracts.

2.2.1. *Top Ladinian datum*

In Figure 6a the top Ladinian (surface 5) is chosen as the datum to illustrate that the Anisian and Ladinian facies and structure are fairly monotonous and relatively uniform in thickness. The top of the Sudair Shale is generally covered by the Nafud Desert and not marked by a cuesta, and so it is only known at three points (Khashm Dolqan by SHD-1 Well, Khabra Halwah, and Al Mudarraj). In the top Ladinian datum cross-section, the top Sudair is most likely represented by surface 1, but it could be surface 2 in the south.

The upper part of the Sudair Shale represents the continental early TST of a sequence that passes to an Anisian late TST (horizon A) culminating in MFS Tr40 (surface 3), above which horizon B represents the Anisian HST. Horizons A and B are well dated by pollens and by *Myophoria goldfussi*, a lamellibranch that commonly inhabited this kind of brackish environment. Horizon C represents a younger shallow-marine cycle that includes MFI Tr50 and is dated as Ladinian by conodonts. A hiatus may occur between Anisian horizon B and Ladinian horizon C and is a candidate for the Tr50 SB.

The upper part of horizon C is marked by a thin Ladinian sequence and capped by a gypsum deposit at Khashm Dolqan. The contrast between the gypsum below and clastics above suggests a hiatus (corresponding to surface 5—candidate for Tr60 SB). The clastics above surface 5 are not dated; they could be latest Ladinian or more likely early Julian. They correspond to a change in clastic influx and climate conditions from arid (gypsum in upper Ladinian) to humid which from Haq [2018], would correspond to the sea level lowstand 237.5 Ma, TLa3 sequence, at the Ladinian-Carnian boundary. When compared with the Alps and the Germanic basin, hiatuses are very likely between the Ladinian evaporite and the Julian clastics [Hornung et al., 2007]. We tentatively assign these clastics to the "Julian Clastic Event".
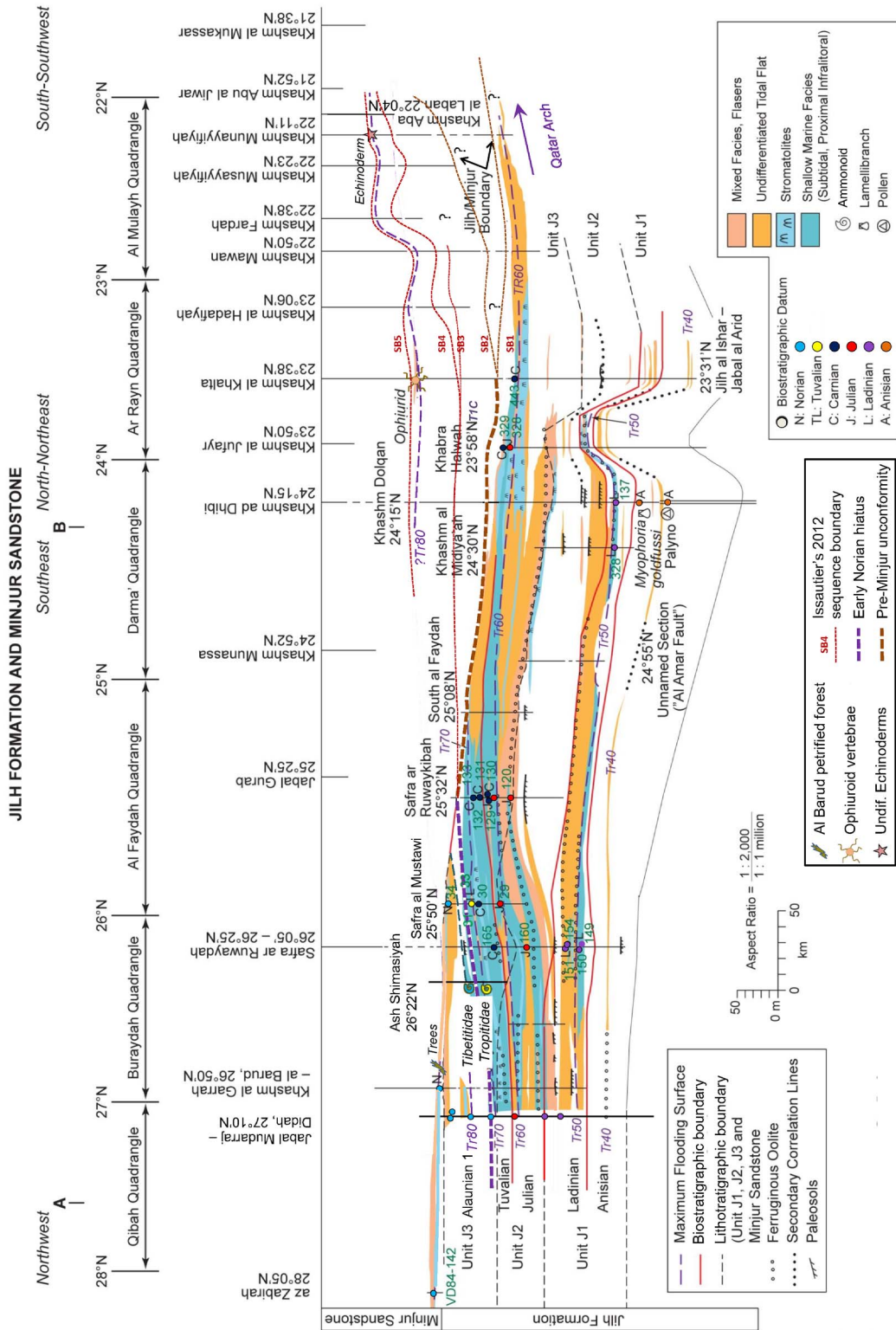
Figure 5. Ages and maximum flooding events of the Jilh–Minjur systems based on marine carbonates stratigraphy.
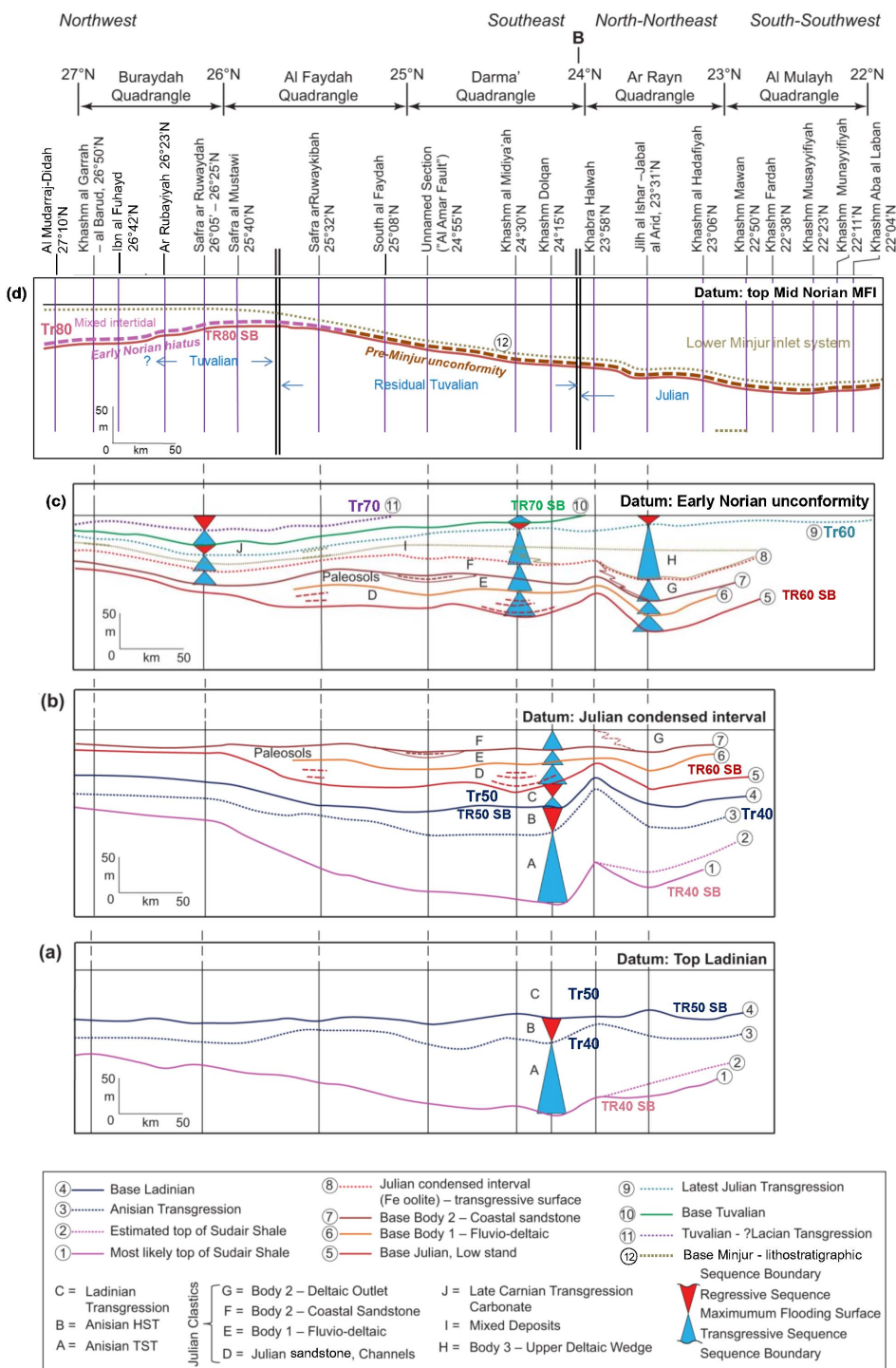
Figure 6. (a)–(d) Stratigraphy of the depositional sequences at four stages of the Jilh Formation sedimentary history.
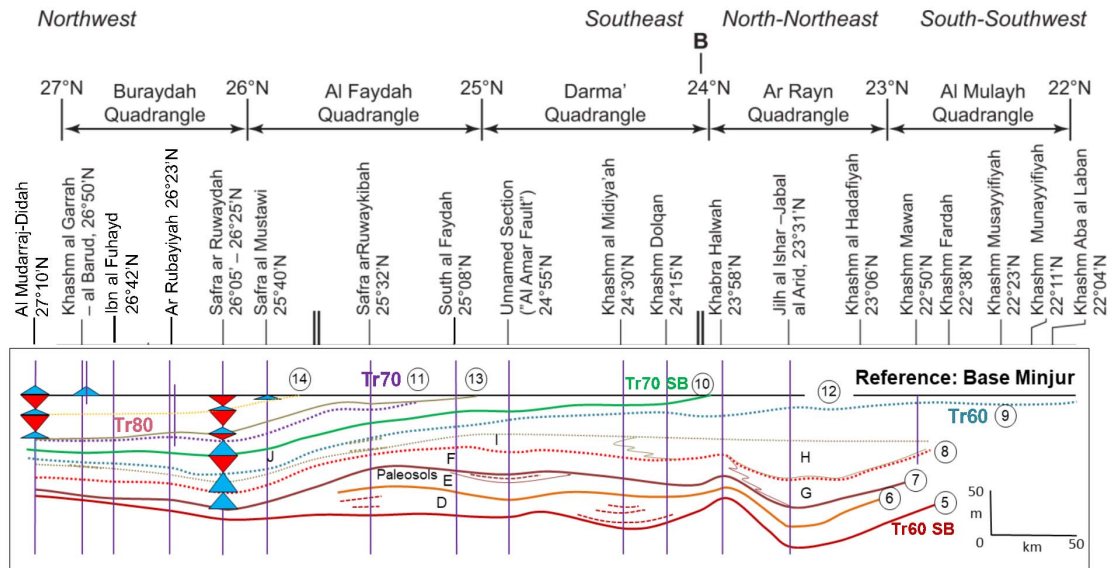
Figure 7. Stratigraphy of the depositional sequences of the Jilh Formation from the late Ladinian-basal Carnian low-stand, horizontalized at the base of Minjur clastics (lithostratigraphic). Letters and numbers refer to the legend of Figure 6(a)–(d). In addition, (13): Early Norian hiatus disconformity surface; (14): intermediate Alaunian tidal sequence boundary.
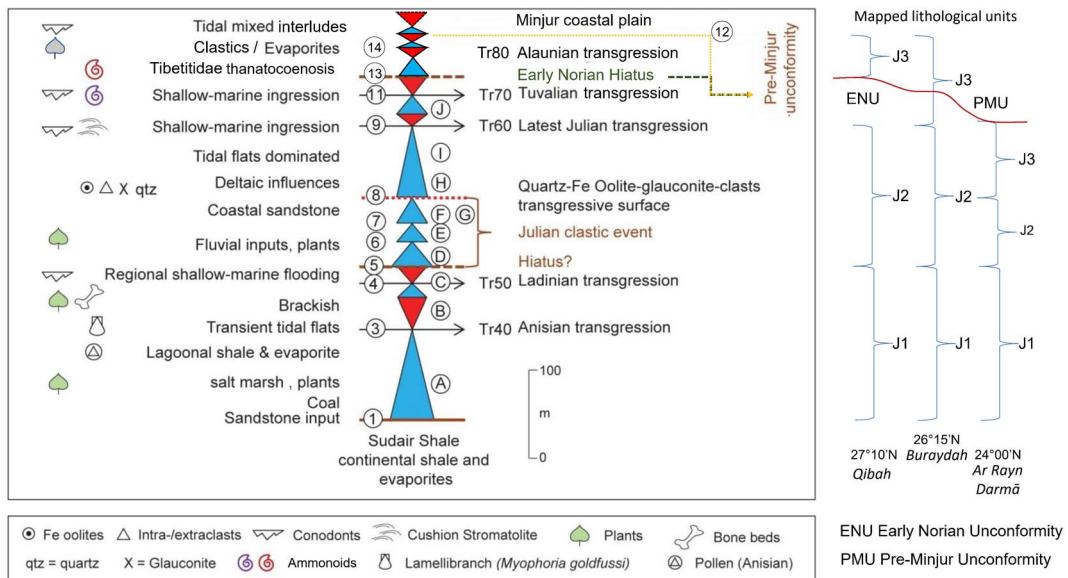

Figure 8. Synthetic sequence stratigraphy of the Jilh Formation in outcrop between latitudes 22° N and 27° N. Surface (12): base of the Minjur Sandstone (lithostratigraphic). Early Norian (pars) present in the Lower Minjur in Central Arabia.
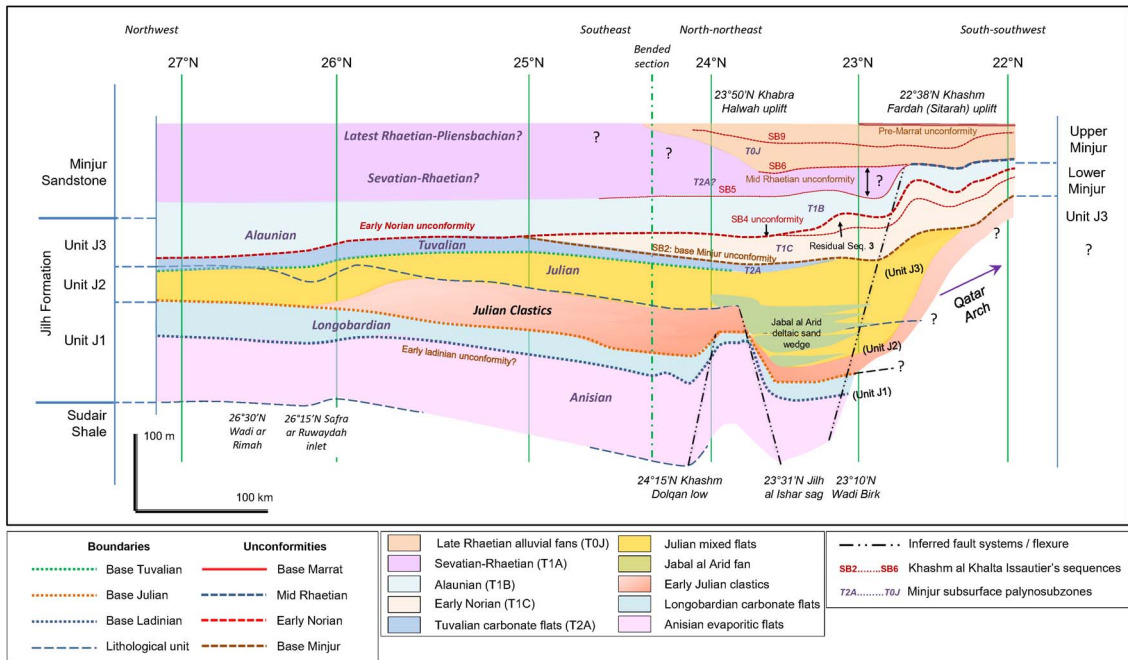
Figure 9. Synthetic conceptual sketch of the Jilh–Minjur systems in outcrop summarising the main structural features, the geometric relationships of the depositional sequences, especially the unconformable Alaunian transgressive wedge.

2.2.2. *During Julian (Time reference: ?mid Julian condensed interval)*

This datum, which we name "Julian condensed interval" (*sensu* Vail's school), is characterized by Fe-oolite (formerly chlorite?), glauconite, quartz and intraclasts with reworked Permian fauna (surface 8, Figure 6b) and estimated by *M. carnica* as ?mid–late Julian. The first observation is the structural change of the previous deposits, related to a tectonic phase predating and/or accompanying the deposition of the clastics (horizons D, E and F), but principally of the two depositional horizons D and E, generally capped by paleosols.

Horizon D is assigned to the Julian and characterized by a landscape of supralittoral shales and creeks with channels of heterometric fluvial sandstone. Sandstone bodies, in channels in horizon D, become aggregated in Julian horizon E. Laterally at Jabal al Arid, horizon E corresponds to the deposition of the first deltaic sandstones [Le Nindre et al., 2023].

Sandstone bodies D and E evolved to Julian sandstone body F by transgression and reworking of the fluvial sandstone to coastal and tidal sandstone, which are extensive, relatively sheet-like and uniform in thickness. Laterally, at Jabal al Arid, a deltaic outlet incises the coastal sandstone (body G). So, this time interval is characterized simultaneously by tectonic structuration and clastic influx, filling lowlands between the structures. At this stage it is difficult to determine if the basal sandstone and change of regime were driven by a sea-level low stand, or principally by a change in clastic influx related to tectonics and climate, or even a combination of these. Therefore, the base of the Julian Clastic Event (surface 5) can be considered as a sequence boundary (presumably Tr60 SB) with a possible hiatus following the Ladinian transgression. A tectonic setting with sandstone bodies infilling the grabens (and carbonates on the flat tops) is also common elsewhere during the Triassic. East of the outcrops, Faqira et al. [2009] interpreted the presence of north–south trending horsts and grabens that developed in response to regional extension during the Triassic. In this study, structures such as Qatar high (south of 21°30′ N), "Khashm Fardah (Sitarah) uplift" [22°38′ N, Le Nindre et al., 1983],

"Jilh al Ishar sag" (23°31′ N) and "Khabrah Halwah uplift" (23°50′ N) control the sedimentation. Lineaments in the basement (N135) or major present valleys as the Wadi Birk (23°10′ N) and the Wadi Ar Rimah (26°30′ N) may reveal syn-sedimentary fault systems, active during the Triassic, and, later on, during the Jurassic [Wadi Birk, Al-Mojel, 2017].

2.2.3. *Carnian–Norian boundary: Early Norian unconformity*

At outcrop, the flat reference taken as base Norian is the disconformity surface (Tr80 SB) dated by the first Norian occurrence within the Jilh Formation (Alaunian 1, early Middle Norian) in the north, or by base Minjur, dated Early to Middle Norian in the centre where part of the Early Norian is demonstrably absent [Issautier et al., 2019] (Figure 6c). The main features raised by this choice of levelling reference are the structure of the deltaic wedge at Jabal al Arid in the south (upper deltaic wedge, body H), and a smooth subsident trough in the north (horizon J) through which the marine transgressions of the latest Julian (surface 9 = MFI Tr60) and Tuvalian (surface 11 = MFI Tr70) progressed from the NNE. Clastic inputs persisted laterally (horizon I) during the deposition of a broad deltaic wedge, clearly visible on DTM and satellite imagery [see Issautier et al., 2012a]. This feature enhances the clastic trough of Jabal al Arid.

In contrast, the central area of Khabra Halwah remained dominated by tidal flats and must have been a very low relief setting. The broader transgression is latest Julian (surface 9) and is detected up to 22° N (tidal flat), with more marine conditions (fossils) northward up to 23°30′. With time, the next transgressions are less and less extensive upwards. The orientation of the outcrop, and consequently of the cross section, shows in fact an oblique view of the transgressive wedges. They appear in a transversal section with a south–north progressive regression of the successive pulses that continued during the Norian (Figure 13). So, this cycle reflects a transgressive system up to the latest Julian transgression (MFS Tr60) followed by a progressive retrogradation of the successive marine pulses via the Late Carnian MFS Tr70 until the Mid-Norian (MFS Tr80) later on, although there is clear southwards truncation of the Tr70 flooding event, indicating regional tectonism (and possibly a concurrent eustatic sea-level low) associated with the base Minjur Formation unconformity identified in Part I (Figure 6c). The evaporites of the northern area mentioned by Sharief [1977, 1986] that overlie surface 11 represent the post-Tr70 Tuvalian–Lacian regression [Sharland et al., 2001].

2.2.4. *During Norian (early Mid Norian Transgressive Interval Tr80)*

Descriptions of the Jilh/Minjur boundary from south to north show a major event generally characterized by lag deposits at outcrop scale. The deposits are most likely related to a peneplain over the previous deposits after uplift (in the south) and subsidence (in the north) of the Jilh Formation. In this interpretation, an erosional unconformity separates the Jilh Formation from the Minjur Sandstone (Figure 6d). Flattening the cross section on top of the Alaunian 1 MFI as interpreted in this study (early Mid Norian Tr80), emphasises that south of 25°35′ N, and especially south of 24° N, the major subsident trough of the Lower Minjur gave way to the main streams and deltaic wedge of the stacked Jilh and Minjur reservoirs of central Arabia. As pointed out by Issautier et al. [2012a], this area was likely a persistently weak tectonic zone. North of 25°35′ N, a shallow-marine trough developed during the subsequent regression within the previously more marine area.

Away from the main upstream source of clastic supply, the unconformity separating the Minjur and Jilh formations is difficult to identify in the more fines-dominated succession to the north, although simple stratigraphic relationships indicate that a cryptic time gap must be present in that area.

From the Al Faydah quadrangle to the north of the Buraydah quadrangle both geological maps [Manivit et al., 1986, Vaslet et al., 1985] and satellite images show an evolution of the Jilh outcrops which spread out in relation with facies changes.

From the base, during the Ladinian, deposition of sandstone and dolomite around 26°13′ N are not observed further south. Near the top, a cuesta, mapped as the uppermost Jilh lithological assemblage on the Buraydah geological map [Manivit et al., 1986] is developed, seemingly conformably overlain by the cover of fine-grained sandstone and shale of the Minjur Sandstone, although a significant time gap is probable. Its facies of grey/yellow argillaceous rocks,

with associated dolomite and evaporites, is similar to the one defined as the Baluti Shale Formation in Iraq [van Bellen et al., 1959–2005] mapped by Ziegler [2001] within the "Carnian to Norian paleogeography, together with the Lower Minjur in a narrow zone of "marginal-marine to shallow-marine clastics" (Figure 13). The presence of this marginal-littoral to shallow marine facies, with the *Tropitidae* fauna, below, and the *Tibetitidae* fauna above, reflects a smooth trough that was penetrated from the north by successive marine ingressions (26°15′ N, "Safra ar Ruwaydah inlet").

The lithological assemblage dated Norian by the conodonts and the ammonoids is thus part of the Lower Minjur, and confirms more marine conditions. The present-day morphological character of Wadi Ar Rimah area is probably related to an ancient deep structural feature that was active from Ladinian to Norian. From MFS Tr60, although interrupted by the Early to Middle Norian unconformity, the depositional system was overall regressive with a culmination during the Rhaetian, associated with a reactivation of the hinterland erosion and creation of alluvial fan and of hyperpycnic bodies.

2.3. *Carnian–Norian back-stepping, progradation, and diachronism*

Coming back to the interpretation of a diachronism of the depositional lithostratigraphic units by J. Manivit and B. Vrielynck [in Le Nindre et al., 1987, DrSc theses, and Le Nindre et al., 1990b, p. 187, Figure 38, and this study, above] it is now possible to decipher this conclusion more clearly. By using the method of the Figure 6a–d, we have flattened the Carnian–Norian deposits at the time of the Minjur "petrified forest"—coarse grained clastics, trunks and wood debris—which reflect a change in climate and tectonics and was taken as lithostratigraphic base of the formation (Figure 7). This event erodes the previous marginal marine deposits.

This representation depicts, besides a diachronic lithostratigraphy, principally the mechanisms it originates from. Following the sea level lowstand at 237.5 Ma, during the Early Carnian, the sequences are essentially transgressive and landward backstepping until the latest Julian Tr60 maximum flooding, reaching up to Lat. 22° N southward. Younger sequences are dominantly regressive and accompanied

by a northward seaward progradation. Thus, MFS Tr60 represents the most prominent transgression, which accords well with the plate-wide correlation of the Jilh, Sefidar and Marker Dolomites.

A similar hypothesis was formulated for the Gulailah Formation in Abu Dhabi by Hu et al. [2015] who divided the Jilh-equivalent Gulailah Formation into Lower and Upper Units, with the lower unit being more layer cake and the upper more regressive. They do not appear to have considered differential erosion beneath a base Minjur Formation unconformity.

The picture is complicated by two superimposed unconformities: the Early Norian hiatus in the marginal marine area (north), and the pre-Minjur erosion, in the fluvial-deltaic domain (south), and principally in the axis of the Minjur inlet [see Issautier et al., 2012a, 2019]. Consequently, it is not possible to determine how far the Tuvalian transgression had reached before truncation by the clastic channels. This configuration is likely due to an uplift of the hinterland during the Early–Mid Norian causing its erosion and thus an increased clastic influx.

Southeastward, in the Rub al Khali Basin of central to eastern Saudi Arabia, Deville de Periere et al. [2022] interpreted that the Late Carnian to Early Norian tectonic pulse that generated the unconformity was responsible for the uplift of paleostructures such as the Qatar Arch and the widespread differential erosion of the Jilh Formation.

3. Synthesis of sequence stratigraphy

The stratigraphic evolution of the Jilh and Minjur Formations along the outcrop belt is summarized in Figure 8, which compiles the elementary sequences described along the steps (a) to (d) on the cross sections. This evolution is summarised below:

Anisian transgression (horizon A): Starting from the continental shales and evaporites of the Sudair Shale, the sequence boundary (surface 1) at the bottom is marked by sand input and coal seams. Then, the Anisian shows a period of transgression through salt marshes, with plants and pollens, lagoonal shales and evaporites, ending with transient tidal flats (MFS Tr40, surface 3).

Anisian regression (horizon B): A more confined, possibly lagoonal, setting represented by brackish

shale and sandstone and the lamellibranch *Myophoria goldfussi* completes the HST of the Anisian cycle.

Ladinian cycle (horizon C): A coarse-grained reworked horizon with plants and vertebrate (reptilian and fishes) bone debris marks the sequence boundary (surface 4 = Tr50 SB). It is followed by a rapid regional shallow-marine flooding with a diversified fauna and algae, well dated by conodonts along the outcrop belt (MFS Tr50). It is followed by a regression leading to gypsum deposits in the reference section. In the Ladinian paleogeography, this event likely corresponds to generalized evaporite deposits and to the end of the first arid period. It may be correlated to the sea level low stand from 238 to 237.5 Ma, TLa3 SB of Haq [2018] and Ogg and Chen [2020].

Julian Clastic Event (horizons D to F, and body G): A sharp change occurs in sedimentary conditions with the beginning of a period of major clastic influx marking the Julian sequence boundary (surface 5 = Tr60 SB). Erosional hiatuses may separate the Julian from the Ladinian as explained above. In a landscape of a littoral plain, several fluvial sequences are stacked: horizons D and E, with coarse-grained sandstone and overturned stratifications, capped by thin lagoonal deposits. With progression of the transgression, the sand brought by the river was reworked into coastal/tidal sandstone (horizon F), interrupted by some distal fluvial/estuarine outlets (body G).

Julian Transgression (body H and horizon I): Following the Julian Clastic Event, the transition from clastic to carbonate is underlined by the "TSF" [Time Specific Facies, Brett et al., 2012, Pavia and Martire, 2015], which marks the ongoing transgression with quartz Fe-oolites, glauconites, and intra/extraclasts (surface 8), and some fauna. Deltaic influences persisted in the Jabal al Arid area (body H), but the overall trend is the generalized expansion of tidal flats and an increasing marine influence (horizon I). During the late Julian, the shallow-marine ingression, dated by conodonts and accompanied by marine fauna and cushion stromatolites, reached its maximum (MFS Tr60, surface 9). It was followed by a brief return to more lagoonal conditions representing the succeeding HST.

Tuvalian transgression (horizon J): Several high-frequency cycles of transgression-regression are recorded in the carbonates of the northern area. They can be considered as part of a new shallow-

marine transgression accompanied by a rich marine fauna including ammonoids, and recorded north of 25° N (MFS Tr70, surface 11). The cycle is completed by a return to restricted conditions during the subsequent HST, though this is variably preserved because of erosion beneath the Early to Middle Norian unconformity (Tr80 SB).

Norian transgressive–regressive cycles: A new short-lived transgressive pulse of limited lateral extent is recorded during the Norian north of 26° N as shown by thin carbonate layers and the presence of Norian marker conodonts. The sequence boundary corresponds to a hiatus, owing to the presence of marker conodonts and of *Tibetitidae* of Alaunian 1 age found in a transgressive horizon not far from the Carnian/Norian boundary. Transient returns to evaporite deposits reflect temporary, higher frequency regressions.

One result of this study is the concept of an early Alaunian wedge, corresponding to the Sequence 4 of Issautier et al. [2019] tentatively correlated in outcrop from latitudes 22° N up to 27° N on the basis of similar ages and of a regional flooding event, assigned herein to MFS Tr80, and which truncates the underlying Minjur Sequences 2 and 3 (SB4 unconformity) (Figure 9). However continuous correlation between north and south remains uncertain between latitudes 25° N and 26° N (Al Faydah quadrangle) where the Minjur Sandstone is covered by aeolian sand.

This chronology is comparable with the one proposed by Korngreen and Benjamini [2010] for the northern Arabian Plate. The Mohilla Formation cited in the paper contains abundant interbedded volcanics which complicates interpretation but even so five low-order (LO) cycles were identified and integrated into a sequence-stratigraphic model with eustatic, tectonic, and differential subsidence components: LO Cycle 1 is Late Anisian (Pelsonian), Cycle 2 is Late Anisian to Longobardian, Cycle 3 is Early Carnian, Cycle 4 is Late Carnian, and Cycle 5 is at the Carnian–Norian transition. However, Cycle 5 is likely missing by erosion in Saudi Arabia and over most of the Arabian Plate, being replaced by the early Norian hiatus, but probably preserved in the Israeli boreholes because of their locations towards the western margin of the Arabian Plate. There is no equivalent to the Minjur Sandstone in Israel because of Late Triassic rift-related uplift, thus the pre-

Minjur unconformity is almost certainly merged with the younger Latest Triassic–Early Jurassic unconformity [End Triassic unconformity of Lunn et al., 2019]. Jurassic volcanics or sediments overlie the incomplete Cycle 5.

As mentioned by Issautier et al. [2012a] the Minjur clastics may originate from a regional uplift of the hinterland related to a thermic dome as modelled by Le Nindre et al. [2003].

4. Particular events and their regional correlations

Jilh sedimentation is marked by important clastic influx, especially during the early Julian alternating with biogenic and chemical deposits such as carbonates and evaporites, following tectonic or global changes. It displays marked lateral facies change into shales, dolomites and anhydrites in the Ghawar area subsurface [Zhou et al., 2009, location on Figures 1 and 12]. Carnian clastics events are well documented in the literature ("Carnian pluvial event"). In contrast, the precise timings of evaporite in the sequence are less well constrained even though Carnian evaporites are common across the Arabian Plate ("Carnian Salinity Crisis"). These alternations are controlled by a combination of tectonic phases, such as the Late Ladinian–Early Carnian rifting, and climate changes which have regional consequences recorded in the sedimentation. Hence, carbonate and evaporite marker horizons can be followed at a plate scale. Thus, the MFS identified in this study (Tr40, Tr50, Tr60, Tr70 and Tr80) should all be readily correlated, except, where eroded beneath regional unconformities. Therefore, in this section we set the early Norian unconformity demonstrated herein in the context of more regional Carnian–Norian hiatuses.

4.1. *Age and cause of the Julian Clastic Event*

Based on structural considerations and on ages of the events described at the Ladinian/Julian boundary in section "Depositional and structural evolution...", above, it seems likely that the Julian Clastic Event and its lateral variations, and probable hiatus between Ladinian and Carnian are related to a second phase of Neo-Tethyan extensional tectonics—first phase at the Permian-Triassic boundary—which occurred during this period in the eastern part of the

Arabian Platform [Le Métour et al., 1995, *in* Ziegler, 2001]. Le Nindre et al. [2003], also invoked a thermal doming causing erosion of the hinterland during the Late Triassic time. Ziegler [2001] also mentions that: "early in the Carnian a very pronounced relative drop in sea level was recorded throughout the circum-Mediterranean region".

Following this rifting phase, a contrast between Late Ladinian marine carbonate below and locally coarse clastic deposits above is observed in the studied area as well as for instance, in the Tarasci section (Taurus autochthon) in Turkey [Assereto and Monod, 1974]. At the scale of the Arabian platform, these Early Julian Clastics likely represent the time gap separating the Ghail Formation, dated Olenekian to Ladinian (-Carnian?), from the overlying Milaha Formation, dated Mid to-Late Norian in the Emirates Musandam [Maurer et al., 2008, Urban et al., 2023].

Later on, field and well descriptions of the Jilh Formation and of the Minjur Sandstone show interfingering of clastics, dolomite, and evaporite. So, both the Julian Clastic Event and Jilh evaporites (see next section "Jilh evaporites") could be partly related to these tectonic events. This interpretation is favoured over one due solely to climate change, as invoked with the Carnian Pluvial Event (CPE) recorded in the Alps and the German Basin for the late Julian or the Julian/Tuvalian boundary [Claudel, 1999, Gaetani, 2010, Somma et al., 2008]. In the Jilh, this interpretation might explain the latest deltaic event (body H of J3), but it does not match the main clastic event which predates *Mazzaella carnica*, and it is contradictory to carbonate dominance during the latest Julian.

However, according to Arche and López-Gómez [2014] the "Carnian Pluvial Event" occurred over large tracts of Central Pangea. It was a short-lived event (>1 Ma), coeval with a marked sea-level fall and active rifting. These authors have identified the CPE in the Iberian Peninsula as a continental clastic wedge forming the Manuel Formation and coeval sediments, in between marine evaporite formations during a marked sea-level drop event; its age is considered to be Julian by palynological and paleogeographic considerations. They propose, for this period, a new correlation of the sediments of the Iberian Peninsula with coeval sediments of Western Europe, NW Africa and Eastern North America, demonstrat-

ing that the geographical extent of the siliciclastic sediments related to the CPE was much larger than accepted before.

4.2. *Jilh Dolomite*

The Jilh Dolomite is a term used to denote a distinctive interval of clean dolomites widely identified from Kuwait to Abu Dhabi, the eastern Rub al Khali Basin and Oman [Deville de Periere et al., 2022, Obermaier et al., 2012]. Davies and Simmons [2018] interpreted it as of Early Carnian age containing their Tr60 MFS, whereas Lunn et al. [2019] correlated it with their "Marker Dolomite" which they consider a plate-wide marker, also identified in Iran, Iraq, Syria and Jordan. Lunn et al. [2019] assigned a Latest Carnian age to the Jilh Dolomite and picked their Tr80 MFS initially at its base, although Lunn [2020] shifted the pick higher to within the unit. Given these published disagreements, we propose to use our new data to provide a more definitive interpretation.

4.2.1. *Definition*

The subsurface "Jilh Dolomite" is characterized as a tight interval of approximately 30 m thick and c. 25 to 75 m beneath the Minjur Sandstone. It has very distinctive wireline responses, sharp, cylindrical, with a low gamma ray, a low porosity, a high sonic velocity, and the grain density of dolomite, facilitating recognition as the regional "Dolomite Marker" in wells (see Section 2, Triassic Stratigraphy of the Arabian Plate).

4.2.2. *Ar Rub al Khali Basin (Saudi Arabia)*

In the central Rub al Khali Basin, Stewart et al. [2016, location on Figure 1] show this tight dolomite interval with an average thickness of c. 30 m. at the boundary with the Minjur sandstones near the Qatar Arch, (although its identification in their well B appears to be in a limestone and may be an older unit), and up to c. 300 feet (91 m) deeper eastward in the basin at the well Lekhwair-70 in Oman (location on Figures 1 and 12). It is eroded on top of the Qatar Arch. The Minjur Sandstone is similarly eroded. Both are unconformably overlain by the Jurassic. Note that the well denoted "A" in central Arabia is Well 143-3 of Issautier et al. [2019].

In the north Rub al Khali Basin, Deville de Periere et al. [2022] show the same horizon, which includes a marine median limestone band, with an average thickness of c. 32 m, and lying c. 115 m beneath the Minjur Sandstone. While they do not present sampling information, Deville de Periere et al. display age interpretations based on palynology that indicate that the Jilh Dolomite is of Carnian, and almost certainly Early Carnian age given the proximity of the underlying Ladinian beds. Along the eastern flank of the Qatar Arch, it is considerably reduced and probably missing by truncation over the Arch itself. The preserved Jilh Formation is immediately overlain by a residual Minjur Sandstone or directly by Jurassic limestone. The most complete section is in their Well L. Comparison with Well G of Stewart et al. identifies this as the same well and therefore located in the Shaybah Field (location on Figure 1).

4.2.3. *Abu Dhabi*

In Abu Dhabi, Taher et al. [2012] in connection with tight gas exploration, present a cross section of the Gulailah (Jilh)–Minjur succession (Location on Figure 1). The Gulailah Formation was deposited in similar environments than the Jilh Formation, and, with marked thickening towards the east-northeast that Taher et al. interpreted as due to progradation into an intrashelf basin rather than differential truncation beneath the base Minjur unconformity. The "Jilh Dolomite" is easily recognized through its typical wireline response with an average thickness of c. 30 m, with a low permeability. The MFS Tr40 50, and 60 can tentatively be identified through the wireline response and by comparison with the Ghawar section of Zhou et al. [2009], respectively at c. 90, 220, and 370 m above the base of the formation. The upper part of the formation is truncated towards the north by the pre-Minjur and pre-Marrat unconformities in relation with the Qatar Arch. In the south, in the wells N and S, the lithological unit above the Tr60 "Jilh Dolomite" and beneath the Minjur (c. 195 m) could be assigned to the Tuvalian (MFS Tr70 at c. 515 m, in part or in totality, by analogy with the northern outcrops of the Jilh Formation. This would be consistent with the interpretations of Davies and Simmons [2018] concerning the equivalent stratigraphy in neighbouring parts of Oman [Obermaier et al., 2012]. Thicknesses are estimated from the isopach map, figure 5 of Taher et al. [2012].

4.2.4. *Central Arabian Basin*

According to Khan et al. [2015], in the Central Arabian Basin, in eastern Saudi Arabia, the "Jilh Dolomite" member forms a 90–100 ft. (27–30 m) thick blocky and laterally persistent unit in the upper part of the Jilh succession, with generally low log porosities of 5–10%, although some higher measured core porosities (up to c. 30%) are recorded. From a Sequence Stratigraphy point of view, using palynological data, they assigned it to the Early Carnian MFS Tr60, which is in accord with the conclusions of the current study.

In the Ghawar good examples are provided by the wells A2 and B3 in the Ghawar area, east-central Saudi Arabia [Zhou et al., 2009]. Here, the "Jilh Dolomite" is easily recognized through a complete set of wirelines. It matches an interval of c. 45 m thick between the horizons JLDM (top Jilh Dolomite) and BJDM (base Jilh Dolomite) and c. 45 m below the Minjur Sandstone.

In the central Arabian Basin, Lunn [2020, his figures 4 and 6], incorrectly interpreted the correlations of the "Jilh Dolomite" in the Minjur cross-section from Issautier et al. [2019, their figure 14].

- First of all, the "Jilh Dolomite" (12 m) was picked in a layered shale–dolomite interval, c. 25 m below the base Minjur whereas the "dolomite marker" appears 50 m deeper, with a sharp contrast in wireline response between shale, above, and dolomite, below.
- This clayey–dolomitic interval was correlated with a dolomitic bed at the base of the Khashm al Khalta section in outcrop. The latter, in fact on top of the Jilh al Ishar–Jabal al Arid Jilh section [23°36′ N, Vaslet et al., 1983] is the "Jilh Dolomite" dated by Le Nindre et al. [1987, 1990b] as Carnian age by the conodont *Quadralella polygnathiformis* [see Part I, Le Nindre et al., 2023 and its Appendix A4], the most landward faunal indicator of the MFS Tr60 in outcrop (see Figure 5).

4.2.5. *Correlations*

The "Jilh Dolomite" or "Dolomite Marker" is identifiable at the scale of the platform, as shown by the "Triassic regional stratigraphic correlation panel Jordan–Syria–Iraq–Lurestan–Kuwait–Saudi Arabia. (Datum: base Marker Dolomite)" of Lunn [2020],

his figure 6. This correlation plate demonstrates that, starting from the outcrop sequence through the Ghawar [Zhou et al., 2009, see above], two major transgressive dolomitic horizons are always present: the (late) Ladinian containing the MFS Tr50, and the late Early Carnian Tr60. Through all these sections, it is interesting to observe that:

- The uppermost dolomite of the section Jilh al Ishar–Jabal al Arid Jilh section (Section A, Part I, 23°36′ N), is the "Jilh Dolomite" in outcrop and is dated of Carnian age by the conodont *Q. polygnathiformis* (see Part I), and the most landward faunal indicator of the MFS Tr60.
- Sequence 1 of Issautier et al. [2012a, 2019] "Transition Jilh–Minjur", above the "Jilh Dolomite" of the Jilh al Ishar–Jabal al Arid section and below the first fluvial beds of the Minjur Sandstone in Khashm al Khalta, may correspond, by its evaporite and clastic content, and by the correlation done, to the intermediate sequence observed in wells [e.g., Sequence 4 of Deville de Periere et al., 2022]. So, it would correspond to a residual, evaporitic, undated Tuvalian, on the basis of a Late Carnian age of this intermediate lithological unit in other wells (T2A palynosubzone).

4.3. *Jilh Evaporites*

In the Middle East, thick Triassic evaporites occur in several formations that are coeval with the Jilh Formation. They are sometimes grouped together as the "Carnian Salt Crisis" [Al-Husseini, 2008, Haq and Al-Qahtani, 2005, Lunn et al., 2019, Sharland et al., 2001, 2004]. These evaporites are referred to as the "Jilh Salt" in subsurface Saudi Arabia, "Middle Salt" in Kuwait, Kurra Chine Salt or Lower Kurra Chine Evaporite in Syria, the Zerqa (Zarqa) Gypsum or Halite in Jordan, and Evaporite members of the Dashtak Formation in Iran. This "salinity crisis" [Hirsch, 1992] expressed itself in the epicontinental regions as a typical lowstand evaporite sequence dominated by halite and sulphate deposition, continental sands, marls and shales. Evidence from the Palymyride Trough in Syria is of very shallow water deposition throughout the thick Triassic section [Lucic et al., 2010], indicating that sedimentation generally maintained pace

with the creation of accommodation space even in areas prone to greater subsidence.

4.3.1. *Surface Saudi Arabia*

Our study indicates that the Jilh Formation in outcrop contains disseminated evaporitic beds rather than a major evaporitic interval clearly differentiated in the stratigraphy as Haq and Al-Qahtani [2005] had suggested in their chart. This is likely due to the proximal outcrop setting which corresponds to a marginal location where siltstone–claystone deposition dominated over evaporites (Figure 3, Part I) which are more concentrated in central or eastern depressions [Glintzboeckel, 1981, Ziegler, 2001]. However horizons with evaporitic or pre-evaporitic facies are observed: (1) in the Anisian of Unit J1; (2), in the Ladinian–?early Julian Unit J1, essentially in the reference section (24°15′ N); (3) in the latest-Julian–?Tuvalian Unit J3 between 24°30° N and 23°30′ N (Khabra Halwah, Khashm al Khalta), and (4) in the Norian Unit J3, north of 26° N. Elsewhere, evaporites occur as thin intercalations within the dolomitic tidal flats and algal mats of sabkha deposits of the formation. In this discussion we review the age interpretations of various evaporitic units in other regions and their relationship to the Jilh outcrop in Central Arabia.

4.3.2. *Subsurface Saudi Arabia*

In subsurface Saudi Arabia, Haq and Al-Qahtani [2005, see their enclosure 2] show the Jilh evaporite in mid-Carnian, immediately pre-dating Tr70, and above the "Lower Jilh", although we would caution that their model was based on the flawed Sharland et al. [2001] interpretation. Comparison with the original definitions in the reference section of the "Lower Jilh" and "Upper Jilh" indicates that the former corresponds to Anisian–Ladinian Unit J1 (Figure 2, Part I). The position of the Jilh evaporite in lowermost Unit J2 strongly implies an early Julian rather than a mid-Carnian age. An early Julian age is in agreement with the age of the "Carnian Salt Crisis" of Ziegler [2001], who related the evaporites to the sealevel lowstand of the early Carnian "Saharan Salinity Crisis". It is also consistent with the Julian age for the "Carnian Salt Crisis" in the Middle East, based on ostracods and palynomorphs determined by Gerry et al. [1990].

The regional vertical distribution of the Jilh Evaporite into four stages is shown by Issautier et al. [2019, their figure 16, p. 166]:

- The Anisian evaporite, predates the dolomite and tidal flats of the transgression Tr40.
- The Mid Ladinian evaporite, corresponds to the coastal plain and sabkha deposits (gypsum silts and clays) underlying Ladinian MFS Tr50 in outcrop (Figure 3, Part I).
- The Late Ladinian–early Julian evaporite corresponds to the gypsum above MFS Tr50 in the reference section at Khashm Dolqan and to the relative lowstand near the base of the Julian clastics. These two episodes are coeval with the coastal plain/sabkha deposits shown in Figure 3, Part I. They occur above and below the Ladinian tidal flats and, together with the Julian clastics, match the Early Carnian Salt Crisis of Ziegler [2001, his figure 5].
- The Tuvalian evaporite is locally observed above the dolomite Tr60, as for instance in Minjur Sequence 1 of Issautier et al. [2012a] which Issautier et al. [2019] correlated with the T2A palynosubzone in the nearest Well 143-3 [Well A of Stewart et al. [2016], location on Figure 1].

In summary, compiling well logs [e.g., Deville de Periere et al., 2022, Lunn, 2020, Zhou et al., 2009] shows that the Jilh evaporites in subsurface Saudi Arabia are commonly interstratified as anhydrite stringers within dolomitic beds between the two major flooding intervals Tr50, Ladinian, and Tr60, Julian ("Jilh Dolomite"), thus time equivalent with the "Julian Clastics", as well as preceding the Ladinian flooding Tr50 and in the Anisian. Anhydrite stringers may also be observed in the Norian portion in equivalence with the Alaunian 1 evaporite described in the field, north of the Wadi ar Rimah (Lat. 26° N, North Wadi ar Rimah and Ibn al Fuhayd sections).

4.3.3. *Northern Arabian Plate*

In the northern Arabian Plate, Sadooni and Alsharhan [2004] described an Anisian–Ladinian "Keuper type" evaporite and an early Carnian "Raibl type" ("Pan-Mediterranean salt crisis"). These evaporites correlate to the Anisian and Ladinian–early Julian

evaporites in the Saudi Arabian outcrops. In the Minagish and Burgan fields in Kuwait (location on Figures 1 and 12), Lunn [2020] mentioned it as "Jilh Salt" in between two major dolomitic intervals which, similarly, corresponds to the same Ladinian and Julian MFI's, referring to current study, Davies and Simmons [2018], and to larger scale correlations.

Equivalences of the Norian evaporite mentioned in the Jilh Formation and at the base of the Minjur Sandstone north of the Wadi ar Rimah (26°30′ N, see Part I, Appendix A1) are not well documented at the regional scale. A likely coeval evaporite restricted to the northern Arabian Basin is mapped by Ziegler [2001, his figure 6]. It is uncertain whether the ?Lacian–Alaunian evaporites represented by Sharland et al. [2004] associated with hiatuses in Jordan (Abu Ruweis Formation) and Syria (Mulussa Formation or in Iraq (Upper Kurra Chine Formation) may be time equivalent.

4.3.4. *Iran*

In the Iranian Zagros, the Dashtak Formation represents the Middle to Late Triassic [James and Wynd, 1965]. Biostratigraphic control is limited. Szabo and Kheradpir [1978] recognised four carbonate–evaporite cycles in the Dashtak Formation that could be correlated the length of the Zagros (e.g., Dashtak-1 and Kuh-e-Siah-1 wells, location on Figures 1 and 12). This four-fold stratigraphic layering continues to be identified in multiple recent publications including Hajian Barzi et al. [2015], Davies and Simmons [2018], Esrafili-Dizaji and Dalvand [2018] and Horbury [2018], demonstrating the utility of these subdivisions.

The sequence stratigraphy of the Dashtak Formation by Sharland et al. [2001, p. 190–191 and their figure 3.22] was revised by Davies and Simmons [2018] and may be correlated with the Jilh Formation at outcrop: the Dashtak Evaporite A corresponds to the Sudair Shale, Evaporite B matches the top of the Anisian sequence. Evaporite C occurs between MFS Tr50 and Tr60 (the Sefidar Dolomite Member, (alias "Jilh Dolomite") and would match the late Ladinian–Early Carnian Julian Clastics and evaporites in Saudi Arabia [Davies and Simmons, 2020, their figure 3]. Anhydrite stringers interstratified in the limestone above Tr70 and below J10SB (Neyriz Formation) are differentially preserved beneath the unconformity truncating the Dashtak Formation, where

the two unconformities identified in this study are superimposed. Hence these stringers are much more likely equivalent to the highstand overlying MFS Tr70 than the Alaunian evaporite present north of the 25°30′ N in outcrop in Saudi Arabia (see Figure 3, Part I).

4.4. *Baluti formation and Carnian–Norian unconformity*

For a better understanding of this Early to Middle Norian time gap, it is worth briefly considering stratigraphic data from the northern Arabian Plate. The Baluti Formation, is mentioned by Ziegler in its paleogeographic map of the Late Triassic (Tr60-J10) as a narrow southward incursion of "shallow marine to marginal marine clastics". Although lying in the Ladinian-Liassic interval, the Baluti Formation was originally accepted as of Rhaetian age, by regional correlation in the Stratigraphic Lexicon of Iraq [van Bellen et al., 1959–2005] and thus not synchronous with the early Mid Norian transgression. However, uncertainty continues with respect to the age of the Baluti shales and recent publications present contradictory interpretations of its regional correlations at the scale of the Arabian Plate. For example, Sharland et al. [2004] positioned the Baluti clastics above an early Norian unconformity, between the Upper Kurrachine Formation (dolomite) and the Butmah Formation, in the late Lacian. In their model, the Baluti Formation predates the Tr80 MFS positioned in the Early Alaunian. This interpretation is not far from the schema proposed for the Jilh–Minjur in our present study but in detail cannot represent the true Baluti Formation as defined by Lunn et al. [2019].

Lunn et al. [2019] commented on the confusion concerning the Baluti shales, noting that the term was not used consistently in outcrop and subsurface sections in northern Iraq. In detail they stated that Sharland et al. [2001] misapplied the term to three separate shales ("Shales 1–3"), According to Lunn [2020], only "Shale 2" corresponds to the true Baluti shales. Palynological data for this "Shale 2" in Well Atrush-1—location on Figure 12—[figure 6 of Lunn et al., 2019], provides a general Carnian age, and show a palynoflora discontinuity in the Lower Sarki Formation between 2155 m (LDO of *Classopollis*, Late Norian) and 2170 m (FDO of *Partitissporites*, Carnian).

Lunn et al. [2019] mentioned a Tuvalian (late Carnian) age based on proprietary data from Jebel Gara in northernmost Iraq, although another palynological study by Hanna [2007], stated a Julian (Early Carnian) age for the basal Baluti at the same locality with a possible Norian age for the uppermost beds of the formation. Azo [2020] also interprets the Baluti shales as being partially of Julian age. Thus, the biostratigraphic data available to date remains equivocal and does not refute our interpretation that the "Marker Dolomite" that underlies the Baluti Formation is older than previously interpreted and of Julian (Early Carnian) age, and therefore equivalent to the Jilh Dolomite of Saudi Arabia and neighbouring countries, as proposed by Lunn et al. [2019]. A further consequence of this interpretation is that the thick carbonate–evaporite cycles that form Kurra Chine B and C, as observed in Jebel Kand-1, are most likely of Ladinian to Julian age, and therefore represent higher frequency events that are only easily recognised in areas of increased sedimentation where rapid subsidence generated significant accommodation space. This has important implications for the regional extent of the source–reservoir–seal combination identified in Kurra Chine B in northern Iraq [Lunn, 2020].

From the figures 1 and 3 of Lunn [2020], the shale portion of the Baluti Formation in subsurface (e.g., wells Jebel Kand-1 and Sheikh Adi-1 near Atrush-1—location on Figure 12) is clearly above the Kurra Chine A Dolomite Marker and evaporite sequence, with a sharp contrast above and below suggesting discontinuities. We have explained above in section "Jilh Dolomite" how this marker corresponds to the Late Julian MFS Tr60. Davies and Simmons [2020] in a discussion of Lunn et al. [2019] suggest the Baluti Formation (Shale 2) may comprise two distinct units: a lower main portion of Carnian (possibly Tuvalian) age—overlying the Kurrachine Formation and representing the highstand above MFS Tr60— and a minor upper portion, of Late Norian (Sevatian age)—underlying the Sarki (= Butmah *sensu lato*) Formation—separated by a major time hiatus. This disconformity—although not pointed out in these papers—appears implicitly above BS.25 as "CRN or NOR" (i.e., "Carnian or Norian", BS.34-35) in the palynological chart of Lunn et al., 2019, their figure 4 [after Hanna, 2007], Jebel Gara section. In this chart, the shale portion of the Baluti Formation strictly corresponds to the Baluti shales of the well logs, while the upper limestone portion corresponds with the Lower Sarki/Butmah of the well logs. Erosional relief on this unconformity, comparable to that identified in Saudi Arabia (this study) means that a more complete Tuvalian section, including beds containing MFS Tr70, is almost certainly differentially preserved across northern Iraq. Further biostratigraphic analysis of the Kurra Chine, Baluti and Sarki Formations, particularly focused on conodonts, in multiple sections is recommended.

5. Paleogeography

From Ladinian to Norian times, the paleogeography of the Arabian shelf was dominated by transitional environments (coastal plain to shallow-marine shelf) and mixed carbonate–clastic–evaporite sediments [Glintzboeckel, 1981, Le Nindre et al., 1990a, Murris, 1981, Ziegler, 2001]. In the western area of the shelf, fine-grained clastics were deposited ("shale": siltstone and claystone with some anhydrite), while mixed carbonates and evaporites dominated in the Gulf area. The main events in proximal areas were: deposition of marginal marine deposits with evaporites during the Anisian, influx of continental clastic to the shelf during the Julian and during the Norian (Lower Minjur Sandstone). Marine transgressions occurred during the Ladinian (Tr50), Late Julian (Tr60) and Tuvalian (Tr70), and to a less extent, during the early Alaunian (Tr80) resulting in deposition of marine carbonates. When compared to sections located in the south, the relative abundance of fauna collected from sections now located further north bears witness to the fact that marine conditions persisted for longer in the north than in the south, and this argues in favour of connections with an open-sea environment to the north (outcrop belt is oblique on the general paleogeographic trends).

5.1. *Connection with the Sephardic Province during the Ladinian*

The Early Triassic global paleogeographic setting [Figure 10, modified after Scotese, 2001, and Blakey, 2003] shows the location of the Arabian Plate on the margin of the Neo-Tethys Ocean. A configuration of barred platform (Zagros, Qatar Arch) with stronger

marine connectivity from the north had already appeared at this time.

The paleobiogeography of the Ladinian conodonts (Figure 11) demonstrates the existence of four different associations [Dercourt et al., 2000a,b, Vrielynck and Cros, 1992, Vrielynck et al., 1994].

A major one—Tethyan type—is restricted to open-marine areas in which the sequences of the northern (Alpine), western (Dinarids, Hellenids), and southern (Taurids) margin were deposited; this pelagic association is also encountered in the facies of the eastern Neo-Tethys as far and beyond as Japan.

The other three associations are encountered in relatively shallow-water facies in (1) Germany, (2) the Sephardic Province, and (3) the Balkans. Geographic separation may account for the differences between conodont associations in the Germanic and Sephardic provinces. The specificity of the Balkan shelf is seen as due to its isolation from the Laurasian Plate. An oceanic buffer (the Paleo-Tethys Ocean) may be invoked, having been more substantial during the Ladinian than during the Pliensbachian [Kazmin et al., 1986, Ricou et al., 1985, 1986].

For the Ladinian, among the species collected in this study, forms belonging to the genus *Pseudofurnishius* are characteristic of the Sephardic Province defined by Hirsch [1972], whereas pelagic Tethyan type conodonts [Bender, 1967, Gedik, 1975, Krystyn, 1983, 2008, Vrielynck, 1980, 1987] are missing. The observed Sephardic biofacies thus appears to be associated with sedimentary conditions such as salinity, water depth (shallow platforms surrounding the Neo-Tethys), and temperature or—as envisaged by Tollmann [1984], and Tollmann and Kristan-Tollmann [1985]—the presence of anti-clockwise currents bounding emergent sectors of the African Plate and hampering colonization of the Arabian shelf by open-sea fauna.

During the Carnian and Norian, the Sephardic and Tethyan conodont provincialism either disappears or has yet to be identified.

Kear et al. [2010a,b] come to a similar conclusion given by the vertebrate assemblages collected from the lower Jilh Unit 1 of which affinities reflect the close proximity of the Arabian region to the Sephardic Province, characterized by a distinct faunal composition. This thesis was developed above in the section "Discussion of Ages" with more emphasis on genera and species present.

5.2. *Jilh time-evolution in the paleogeography of the Arabian Plate*

Glintzboeckel [1981, BRGM internal report] drew a series of palaeogeographic maps of Saudi Arabia that included the Middle to Late Triassic stratigraphy described herein. Ziegler [2001] drew, with the input of two of the present authors (YML and DV), two paleogeographic maps corresponding to the Middle to Late Triassic, although still without the full benefit of our current stratigraphic understanding, in particular the importance of the Late Carnian to Early Norian hiatus. In detail Ziegler's two maps depicted composite representations of:

- the paleofacies of the Middle Triassic spanning the deposition of the Jilh Formation and of its regional equivalents from MFS Tr40 to intra- Tr60 (his figure 5);
- the paleofacies of the Late Triassic spanning the deposition of the Upper Jilh and of the Minjur Sandstone from MFS Tr60 to intra-MFS J10 (his figure 6). It can be argued that this latter map is more representative of the Carnian sediments preceding the hiatus in the northern half of the Arabian Plate (e.g., Carnian evaporites in the Palmyride Trough), but of the Norian sediments postdating the hiatus in the southern half, including the outcrops that are the main subject of the present study.

Transposing the facies limits from a N–S section (see Figure 6) to these maps highlight the horizontal dynamics and illustrates the evolution of the transgressions from Ladinian to Norian as visible in the Jilh Formation outcrops, and thus after truncation by the pre-Minjur unconformity (Figure 12).

During the Ladinian and the Lower Carnian (Figure 12), it illustrates the difference of trends between the clastic inputs (towards the northeast) and the marine incursions (from the north), consistent with the migration of Ladinian conodonts from the Sephardic Province. (See Section 5.1. "Connection with the Sephardic Province during the Ladinian" above). Evaporitic pans are concentrated in the Central Arabian Basin. The first stage of transgression corresponds to the southward extent of the Ladinian tidal flats (1) associated with MFS Tr50. Then, during the Early Carnian, clastic wedges prograded from the
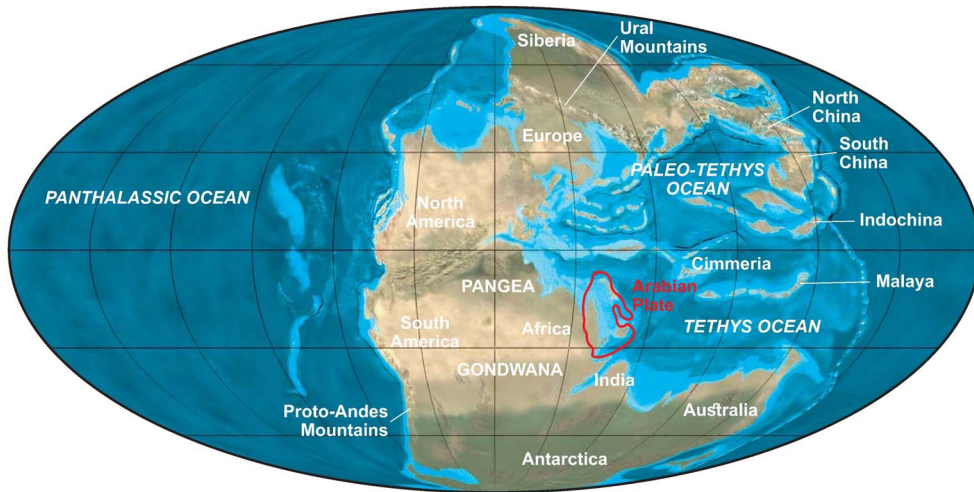
Figure 10. Early Triassic plate-tectonic setting showing the position of the Arabian Plate (in red) with northward opening of the Central Arabia Basin [modified from Scotese, 2001; Blakey, 2003].
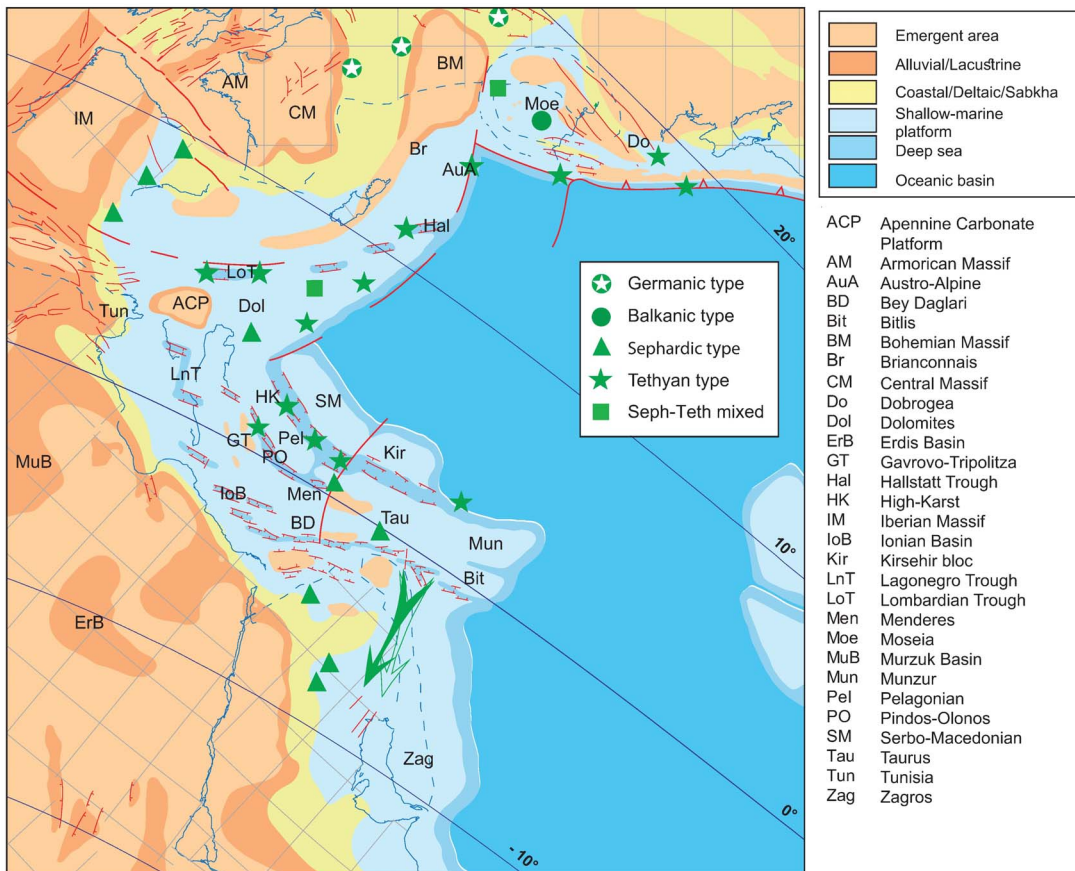

Figure 11. Distribution of Ladinian conodonts throughout the Mediterranean Tethyan domain [palaeo-geographical base-map modified from Dercourt et al., 2000a,b, Barrier and Vrielynck, 2008].
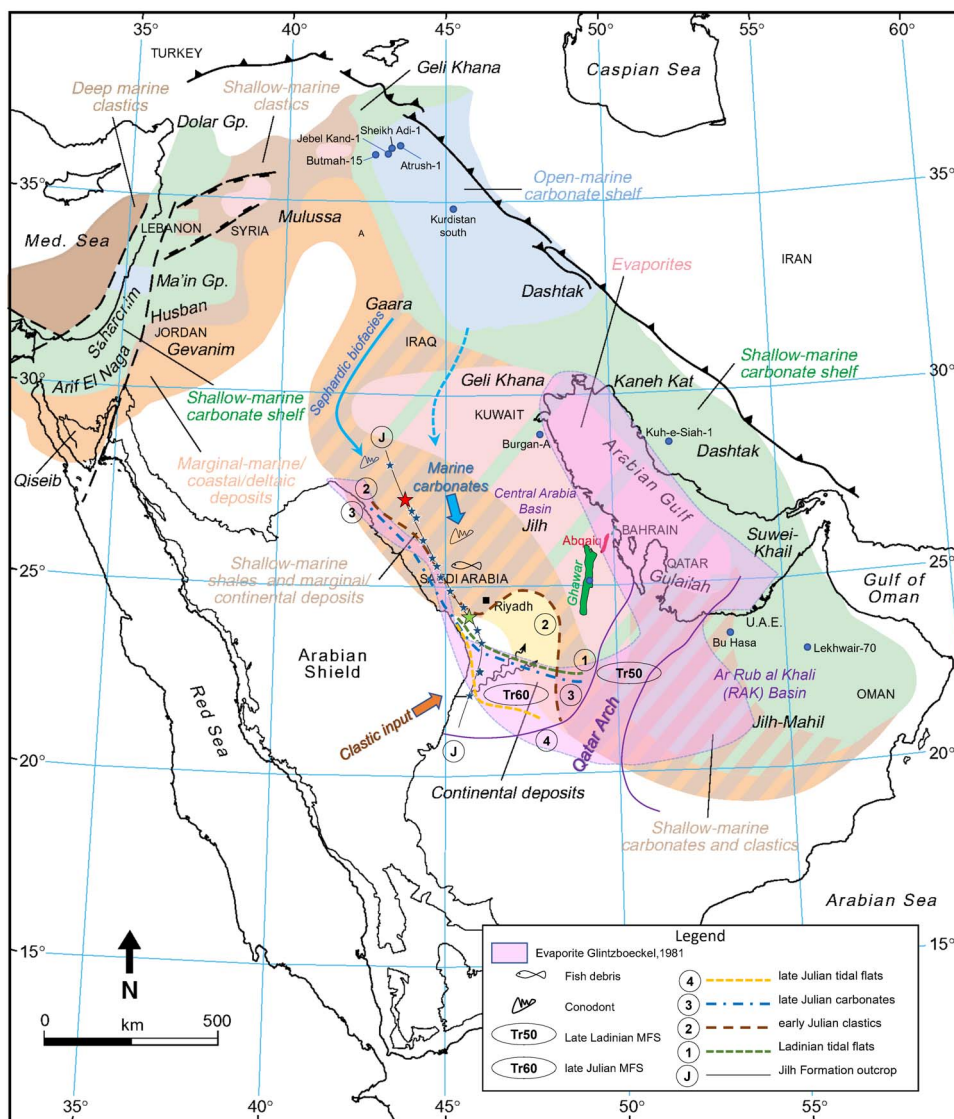
Figure 12. Extent of the main sedimentary events of the Jilh Formation, from Ladinian to late Julian in chronologic order, as in outcrop, and inferred under the early Norian–pre-Minjur unconformity. Base map modified after Ziegler [2001] by permission of GeoArabia, with contribution of Le Nindre et al. [1990a] for the outcrop. Legend for outcrop, see Figure 1.

shelf (2 in Figure 12). During the Julian, the shallow-marine facies (3) achieved their maximum extent southward (23°30′ N) since the Ladinian; meanwhile generalized tidal flats (mixed or carbonated) capped the clastics further south up to 22° N (4, MFS Tr60, Figure 12). Glintzboeckel [1981] depicted more common evaporites in the Gulf, while marine carbonates occupied a broader surface in the north central area,

whereas Ziegler [2001] maps a mixed evaporites and shallow marine carbonate shelf which is more consistent with our present knowledge. In a further difference between the two accounts, Ziegler maps shallow marine carbonates and clastics in the Rub al Khali Basin, while Glintzboeckel extended evaporites into this basin, which is principally true during the Anisian, and partially true during the Carnian [Dev-

ille de Periere et al., 2022].

During the Tuvalian and the Norian (Figure 13), the general shape we give to the transgressive wedges is inspired from the tongue of "Marginal-marine to shallow-marine clastics" (Baluti Formation facies) which penetrates the "continental deposits" during the Norian.

The Tuvalian transgression (5), likely truncated, reached up to 25° N, a little more with tidal flats, and likely up to 23°30′ N: Issautier et al. [2012a] and Issautier et al. [2019] have supposed that the Tuvalian (Tr70) may have a more southern extension at the base of the "Minjur Sandstone" *sensu* Vaslet et al. [1983] at least up to 23°30′ N with sabkha facies (Sequence 1), and in the near subsurface upper Jilh of the well 143-3 (Palynozone T2-A,) but any more southerly extent was truncated by the Carnian–Early Norian unconformity (SB2, Figure 9). The Norian marine deposits (Tr80) reached more or less 25°30′ N southward in the Jilh Formation while tidal flats and local tidal inlet are identified up to 23°30 in the Minjur Formation. The Ladinian to Norian transgressive pulses appear with the marine influences progressively regressing northwards in relative to the central evaporitic basin. This Norian paleogeography is consistent with the global Neo-Tethys reconstruction for this period of Berra and Angiolini [2014].

6. Conclusions

(1) New correlations within the Jilh Formation and the Minjur Sandstone in outcrop and subsurface highlight geometric and chronostratigraphic aspects of the Middle–Late Triassic in Saudi Arabia.

(2) Five main marine flooding intervals characterizing the late Mid–Late Triassic Epochs were demonstrated from outcrops on the western margin of the Arabian shelf. It is likely that the Anisian tidal flats deposits represent the MFS Tr40. The other marine flooding events are well constrained by marker faunas: Ladinian MFS Tr50, late Julian (Early Carnian) MFS Tr60, Tuvalian (Late Carnian) MFS Tr70, and early Alaunian (Mid Norian). Different populations of Ladinian conodonts in stratigraphically equivalent horizons are explained by environmental factors, instead of age differences. La-

cian rocks are probably absent owing to erosion beneath the combined Late Carnian to Early Norian and Early to Middle Norian unconformities [SB2 and SB4 respectively, of Issautier et al., 2012a, 2019]. The Alaunian MFS (S4 MFS) is, dated by *Tibetitidae* and the *Ancyrogondolella praeslovakensis* faunas, north of Lat. 25° N, in correspondence with the *Rhaetogonyaulax wigginsii* palynosubzone of the middle Minjur. It is tentatively assigned to "Tr80" in Central Arabia. An alternative definition of "Tr80" exists in Musandam in the Milaha Formation [Davies and Simmons, 2018], but the most recent results from that section [Urban et al., 2023] appear to favour a similar Middle Norian age for this MFS, with a Late Norian age for the overlying sequence in the Ghalilah Formation (MFS Tr90?).

(3) Truncations separating the packages could be invoked at the base of the Julian clastics (base Unit J2), at the base of the Late Julian transgression (TSF, Time Specific Facies— Brett et al., 2012, Pavia and Martire, 2015— with Fe oolites) on top of paleosols, and between the Carnian and the Norian. These are candidates for plate-wide sequence boundaries (Tr60 SB, Tr70 SB and Tr80 SB). The nature of the boundary between the Anisian and the Ladinian is not definitively resolved at the regional scale.

(4) The boundary between the Jilh Formation and the Minjur Sandstone [SB2 of Issautier et al., 2012a, 2019] is sharp, with an erosional contact in the fluvial portion of the system in central Arabia near the reference sections. Towards the south, a valley fill containing tidal inlet, sabkha, and fluvial deposits is identified. An undated sequence [Minjur Sequence 1 of Issautier et al., 2012a,b] with sabkha facies previously assigned to the Minjur Sandstone caps the Julian Jilh Dolomite and underlies these erosional channels. By lateral correlation we have interpreted these horizons as residual Tuvalian (T2A palynosubzone). An important finding of this study is reconstruction of an early Alaunian transgressive wedge, with an erosive base taken on the sequence boundary (SB4) which
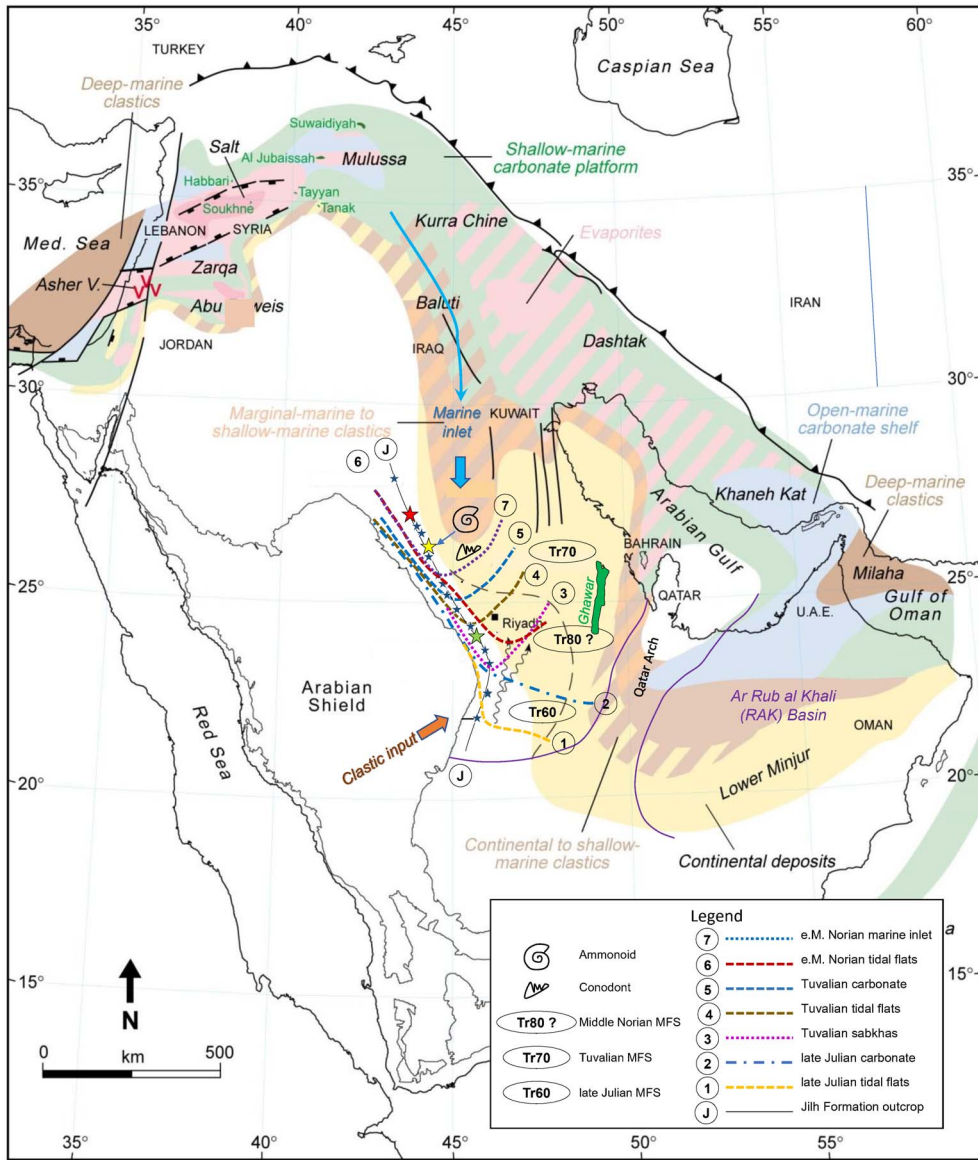
Figure 13. Extent of the main sedimentary events of the Jilh Formation, from late Julian to Middle Norian in chronologic order, as in outcrop, and inferred under the early Norian–pre-Minjur unconformity. Base map modified after Ziegler [2001] by permission of GeoArabia, with contribution of Le Nindre et al. [1990a] for the outcrop. For legend of the Jilh outcrop, see Figure 1.

had been correlated from central to north Arabia.

(5) Interfingering of various sediment types, and abrupt changes in lithology, as at the Ladinian Carnian boundary, are not explained by sea level changes alone. The deconstruction done, employing multiple datums, illustrates the role of tectonics, by identifying several structures active during the sedimentation. This does not exclude a probable, though possibly minor, role of the climate, including the Carnian Pluvial Event. This study enables a better understanding of the complex relationships between carbon-
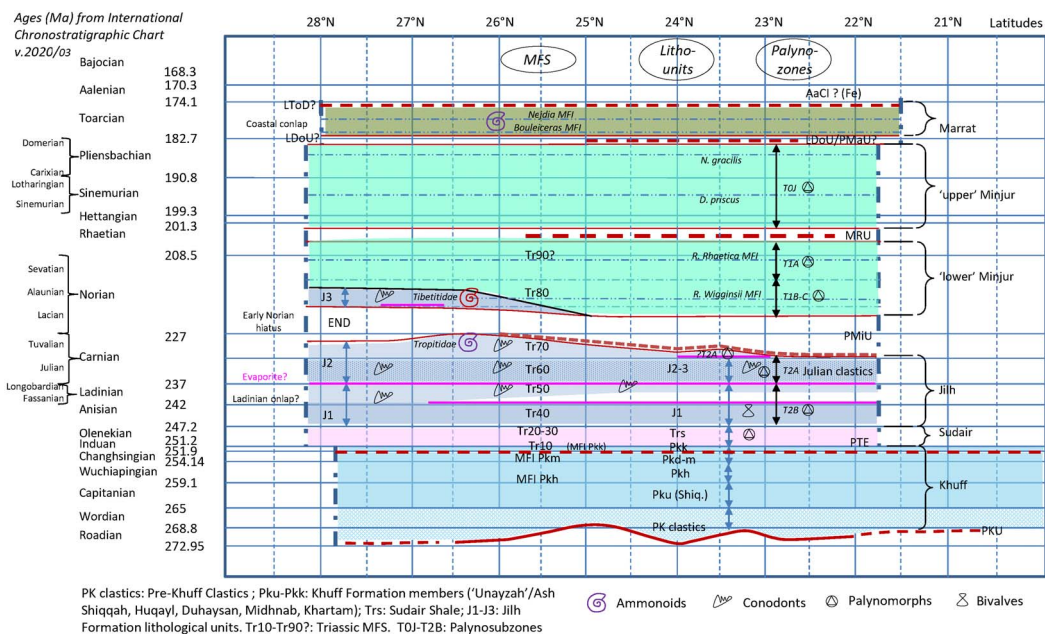
Figure 14. Overall chronostratigraphic chart of the Late Permian to Mid Toarcian time interval. MFS modified after Davies and Simmons [2018]; Permian and Triassic depositional units after Le Nindre et al. [1990b] and Vaslet et al. [2005]; palynozones after Issautier et al. [2019] and Deville de Periere et al. [2022]. (PKU: Pre-Khuff unconformity; END: Early Norian disconformity; PMiU: Pre Minjur unconformity; MRU: Mid Rhaetian unconformity; LDoU?/PMaU: Domerian/Pre-Marrat unconformity; LToD: Late Toarcian disconformity; AaCi (Fe): Aalenian condensed interval.)

ate, evaporites and siliciclastic detrital rocks which are the major characteristic of these Mid–Late Triassic Epochs. Through a stratigraphic analysis based, not just on well logs facies correlation but on reliable biostratigraphic studies in outcrop (to be continued), better regional correlations are made possible.

(6) The paleogeographic reconstruction first inserts the faunas collected for the study in a Tethyan paleo-biogeography. Understanding their migration is a precious aid to reconstruction of the processes of transgression and regression at large scale. The lessons learned from outcrop are now integrated in the Middle East paleogeography of the Mid–Late Triassic, showing the dynamic keys of the different periods.

(7) From the results obtained in Parts I and II of this study, complemented by previous publications [e.g., Davies and Simmons, 2018, Deville de Periere et al., 2022, Haq, 2018, Is-

sautier et al., 2019, Le Nindre et al., 1990b, 2022, 2023, Manivit et al., 1990, Vaslet et al., 2005], we have derived an overall chronostratigraphic chart spanning this time interval and expanded to include the Late Permian to Early Triassic Khuff Formation and Sudair Shale, and the Early Jurassic Marrat Formation (Figure 14). The absolute ages are from GTS 2020/03 [Cohen et al., 2013, updated 2020]. These results facilitate correlation throughout the platform, especially where reliable biostratigraphic markers are present.

Conflicts of interest

Authors have no conflict of interest to declare.

Acknowledgments

References

Al-Husseini, M. I. (2008). Launch of the middle east geologic time scale. *GeoArabia*, 13(4), 185–188. p. 11.

Al-Mojel, A. S. (2017). *Sedimentology and Sequence Stratigraphy of the Jurassic, Jabal Tuwaiq, Central Saudi Arabia*. Thesis 2017 bor30037, Doctorate Sciences and Technology, Université Bordeaux Montaigne. 01/12/2017, 368 p., 87 figures.

Arche, A. and López-Gómez, J. (2014). The Carnian Pluvial event in Western Europe: new data from Iberia and correlation with the Western Neotethys and Eastern North America–NW Africa regions. *Earth-Sci. Rev.*, 128, 196–231.

Assereto, R. and Monod, O. (1974). Les formations triassiques du Taurus occidental à Seydischir (Turquie méridionale). Stratigraphie et interprétation sédimentologique. *Memorie Riv. Ital. Paleon-tol. Stratigr.*, 14, 159–191. Milano Italy. ISSN 0035-6833, online ISSN 2039-4992.

Azo, N. M. (2020). *Palynology of the Baluti Formation (Upper Triassic) in two selected sections at Amediya District, Kurdistan Region, Iraq*. Unpublished msc thesis, Soran University, Iraq. 147 p., 16 Plates.

Barrier, E. and Vrielynck, B. (2008). Palaeotectonic maps of the Middle East. In *Tectono-sedimentary-palinspastic Maps from Late Norian to Pliocene*, Commission for the Geological Map of the World (CGMW/CCGM). Commission de la Carte Géologique du Monde, Paris. ISBN 9782917310007, 14 maps.

Bender, H. (1967). Zur Gliederung der mediterranen Trias. II; Die Conodontchronologie der mediterranen Trias. *Ann. Géol. Pays Helléniques*, 19, 465–540.

Berra, F. and Angiolini, L. (2014). The evolution of the Tethys region throughout the Phanerozoic: A brief tectonic reconstruction. In Marlow, L., Kendall, C., and Yose, L., editors, *Petroleum Systems of the Tethyan Region*, AAPG Memoir 106, pages 1–27. AAPG, Tulsa, Oklahoma.

Blakey, R. C. (2003). Carboniferous–Permian paleogeography of the assembly of Pangaea. In Wong, T. E., editor, *Proceedings of the XVth International Congress on Carboniferous and Permian Stratigraphy, Utrecht, the Netherlands, 10–16 August 2003*, pages 443–456. Royal Netherlands Academy of Arts and Sciences.

Brett, C. E., McLaughlin, P. I., Histon, K., Schindler, E., and Ferretti, A. (2012). Time-specific aspects of facies: State of the art, examples, and possible causes. *Palaeogeogr. Palaeoclimatol. Palaeoecol.*, 367–368, 6–18.

Claudel, M.-E. (1999). *Reconstitution paléogéographique du domaine briançonnais au Mésozoïque. Ouvertures océaniques et raccourcissements croisés*. PhD thesis, Université Joseph-Fourier – Grenoble, France.

Cohen, K. M., Finney, S. C., Gibbard, P. L., and Fan, J. X. (2013). The ICS International Chronostratigraphic chart. *Episodes*, 36, 199–204. http://www.stratigraphy.org/ICSchart/Chronostratchart2020-03.pdf.

Davies, R. B. and Simmons, M. D. (2018). Triassic sequence stratigraphy of the Arabian Plate. In Pöppelreiter, M. C., editor, *Lower Triassic to Middle Jurassic Sequence of the Arabian Plate*, pages 101–162. EAGE Publications B.V., The Netherlands.

Davies, R. B. and Simmons, M. D. (2020). Dating and correlation of the Baluti Formation, Kurdistan, Iraq: implications for the regional recognition of a Carnian "marker dolomite" and a review of the Triassic to Early Jurassic sequence stratigraphy of the Arabian Plate by G. A. Lunn, S. Miller and A. Samarrai. Discussion. *J. Pet. Geol.*, 43(I), 95–108.

Davies, R. B., Simmons, M. D., Jewell, T. O., and Collins, J. (2019). Regional controls on siliciclastic input into Mesozoic depositional systems of the Arabian Plate and their petroleum significance. In AlAnzi, H. R., Rahmani, R. A., Steel, R. J., and Soliman, O. M., editors, *Siliciclastic Reservoirs of the Arabian Plate*, AAPG Memoir 116, pages 103–140. AAPG, Tulsa, Oklahoma.

Dercourt, J., Gaetani, M., and Vrielynck, B. (2000a). General features of the atlas. In Crasquin, S., editor, *Atlas Peri-Tethys, Palaeogeographical Maps*, pages XI–XX. CCGM/CGMW, Paris. Explanatory notes.

Dercourt, J., Gaetani, M., Vrielynck, B., Barrier, E., Biju-Duval, B., Brunet, M. F., Cadet, J. P., Crasquin, S., and Sandulescu, M., editors (2000b). *Atlas Peri-Tethys, Palaeogeographical Maps*. CCGM/CGMW, Paris. 24 maps, 269 p.

Deville de Periere, M., Breuer, P., Alsinan, F., and Lu, F. (2022). Sedimentology, sequence stratigraphy, palynology, and diagenetic evaluation of the Triassic Jilh Formation. New insights from Saudi Arabia. *J. Afr. Earth Sci.*, 196, article no. 104714.

Esrafili-Dizaji, B. and Dalvand, M. (2018). Early–middle triassic dashtak formation in the zagros domain. In Pöppelreiter, M. C., editor, *Iran: Controls of Eustasy, Tectonic, and Palaeoclimate*, Lower Triassic to Middle Jurassic Sequence of the Arabian Plate, pages 163–178. EAGE Publications B.V., The Netherlands.

Faqira, M., Rademakers, M., and Afifi, A. M. (2009). New insights into the Hercynian Orogeny, and their implications for the Paleozoic Hydrocarbon System in the Arabian Plate. *GeoArabia*, 14(3), 199–228.

Furin, S., Preto, N., Rigo, M., Roghi, G., Gianolla, P., Crowley, J. L., and Bowring, S. A. (2006). High-precision U-Pb zircon age from the Triassic of Italy: Implications for the Triassic time scale and the Carnian origin of calcareous nannoplankton and dinosaurs. *Geology*, 12, 1009–1012.

Gaetani, M. (2010). From Permian to Cretaceous: Adria as pivotal between extensions and rotations of Tethys and Atlantic Oceans. *J. Virtual Explor.*, 36, article no. 6. (Electronic Edition). In (Eds.) M. Beltrando, A. Peccerillo, M. Mattei, S. Conticelli, C. Doglioni, The Geology of Italy: tectonics and life along plate margins.

Gedik, I. (1975). Die Conodonten der Trias auf der Kocaeli-Halbinsel (Türkei). *Paleontogr. Abt. A.*, 150, 99–160.

Gerry, E., Honigstein, A., Rosenfeld, A., Hirsch, F., and Eshet, Y. (1990). The Carnian Salinity Crisis, Ostracods and Palynomorphs as Indicators of Palaeoenvironment. In Whatley, R. C. and Maybury, C., editors, *Ostracoda and Global Events (Conference Paper, International Symposium on Ostracoda 10; 1988)*, British Micropalaeontological Society, Publication Series, pages 87–97. Chapman and Hall, New York. Chapter 6, 5 fig.

Glintzboeckel, C. (1981). A tentative synopsis of the Geology of the Saudi Arabian sedimentary basin in relation to phosphate prospecting. D.M.M.R. Jeddah, Open File Report BRGM OF-01- 23, 145 p, 59 fig., 3 tabl.

Gradstein, F. M., Ogg, J. G., Schmitz, M., and Ogg, G. (2012). The Geologic Time Scale. *Newsl. Stratigr.*, 45(2), 171–188.

Hajian Barzi, M., Aleali, M., Jahini, D., and Falahkheyrkhah, M. (2015). Microfacies, sedimentary environment, sequence stratigraphy and strontium dating of the dashtak formation in the Persian Gulf, Fars and Izeh Regions. *Geosciences*, 24, 185–198.

Hanna, M. T. (2007). *Palynology of the upper part of the Baluti Formation (Upper Triassic) and the nature of its contact with the Sarki formation at Amadiya district, northern Iraq.* PhD thesis, University of Mosul, Iraq. 219 p.

Haq, B. U. (2018). Triassic eustatic variations reexamined. *GSA Today*, 28(12), 9. with supplement online at www.geosociety.org/datarepository/2018/.

Haq, B. U. and Al-Qahtani, A. M. (2005). Phanerozoic cycles of sea-level change on the Arabian Platform. *GeoArabia*, 10(2), 127–160.

Hirsch, F. (1972). Middle Triassic conodonts from Palestine, southern France, and Spain. *Mitt. Gesellschaft Geologie Berganstudien*, 21, 811–828.

Hirsch, F. (1992). Circummediterranean Triassic eustatic cycles. *Israeli J. Earth Sci.*, 40, 29–33.

Horbury, A. (2018). Petroleum Geology and its relation to Stratigraphic Architecture of the Triassic

to Middle Jurassic (Induan to Aalenian) Interval on the Arabian Plate. In Pöppelreiter, M. C., editor, *Lower Triassic to Middle Jurassic Sequence of the Arabian Plate*, pages 49–100. EAGE Publications B.V., The Netherlands.

Hornung, T., Bradner, R., Krystner, L., Joachimski, M. M., and Keim, L. (2007). Multistratigraphic constraints on the New Tethyan "Carnian Crisis". In Lucas, S. G. and Spielmann, J. A., editors, *The Global Triassic*, New Mexico Museum of Natural History and Science Bulletin 41, pages 59–67. New Mexico Museum of Natural History and Science, New Mexico.

Hu, J., Witte, J., and Neves, F. (2015). Evolution of the Middle-Triassic Gulailah intra-shelf basin in Abu Dhabi, Abu Dhabi Natonal Oil Company (ADNOC). In *Abu Dhabi International Petroleum Exhibition and Conference, Abu Dhabi, UAE, 9–12 November 2015*, Society of Petroleum Engineers SPE-177586-MS. SPE, Texas. 6 p. 19 figures.

Issautier, B. (2011). *Estimation de l'impact des hétérogénéités sédimentaires fluviatiles sur le stockage géologique du CO$_2$*. Thesis, Université de Provence, Aix-Marseille I. 2011AIX10136 Geosciences de l'Environnement. Geology of carbonate systems and reservoirs, E.A. 4234. 20 December 2011, 152 p.

Issautier, B., Le Nindre, Y. M., Hooker, N., Reid, C., Memesh, A., and Dini, S. (2019). Depositional environments, age, and sequence stratigraphy of the Minjur Formation in outcrop and near subsurface–Central Saudi Arabia. In Al-Anzi, H. R., Rahmani, R. A., Steel, R. J., and Soliman, O. M., editors, *Siliciclastic Reservoirs of the Arabian Plate*, AAPG Memoir 116, pages 141–184. AAPG, Tulsa, Oklahoma. Chapter 5.

Issautier, B., Le Nindre, Y. M., Memesh, A., Dini, S., and Viseur, S. (2012a). Managing clastic reservoir heterogeneity, I: Sedimentology and sequence stratigraphy of the Late Triassic Minjur Sandstone at the Khashm al Khalta type locality, Central Saudi Arabia. *GeoArabia*, 17(2), 17–56.

Issautier, B., Le Nindre, Y. M., Viseur, S., Memesh, A., and Dini, S. (2012b). Managing clastic reservoir heterogeneity II: Geological modeling and reservoir characterisation of the Minjur Sandstone at the Khashm al Khalta type locality (Central Saudi Arabia). *GeoArabia*, 17(3), 61–80.

James, G. A. and Wynd, J. G. (1965). Stratigraphic nomenclature of the Iranian Oil Consortium Agreement Area. *Am. Assoc. Pet. Geol. Bull.*, 49, 2182–2245.

Kadar, A. P., De Keyser, T., Neog, N., Karam, K. A., Le Nindre, Y.-M., and Davies, R. B. (2015). Calcareous nannofossil zonation and sequence stratigraphy of the Jurassic System, onshore Kuwait. *GeoArabia*, 20(4), 125–180.

Kazmin, V., Ricou, L. E., and Sborshchikov, I. M. (1986). Structure and evolution of the passive margin of the eastern Tethys. *Tectonophysics*, 123, 153–179.

Kear, B. P., Rich, T. H., Vickers-Rich, P., Ali, M. A., Al-Mufarrih, Y. A., Matiri, A. H., Masary, A. M., and Halawani, M. A. (2010a). A review of aquatic vertebrate remains from the Middle–Upper Triassic Jilh Formation of Saudi Arabia. *Proc. R. Soc. Victoria*, 122(1), 1–8. ISSN 0035-9211.

Kear, B. P., Rich, T. H., Vickers-Rich, P., Ali, M. A., Al-Mufarrih, Y. A., Matiri, A. H., Masary, A. M., and Halawani, M. A. (2010b). First Triassic lungfish from the Arabian Peninsula. *J. Paleontol.*, 84, 137–140.

Khan, S., Al-Eid, G., Reid, C., Hooker, N., Ertug, K., and Tang, D. (2015). *EAGE 5th Arabian Plate Geology Workshop, Lower Triassic to Middle Jurassic Evaporite–Carbonate–Siliciclastic Systems of the Arabian Plate (Sudair to Dhruma and Time Equivalent), 8–11 February 2015, Kuwait.*

Korngreen, D. and Benjamini, C. (2010). The epicontinental subsiding margin of the Triassic in Northern Israel, North Arabian Plate. *Sediment. Geol.*, 228(1–2), 14–45.

Krystyn, L. (1983). Das Epidaurus-Profil (Griechenland). Ein Beitrag zur Conodonten- Standardzonierung des thethyalen Ladin und Unterkarn. *Oesterr. Akad. Wiss. Schriftenreihe Erdwissenschaften*, 5, 231–258.

Krystyn, L. (2008). An ammonoid-calibrated Tethyan conodont time scale of the late upper Triassic. *Berichte Geol. B.-A.*, 76, 9–11. ISSN 1017-8880 — Upper Triassic . . . Bad Goisern (28.09–02/10/2008).

Le Métour, J., Michel, J. C., Béchennec, F., Platel, J. P., and Roger, J. (1995). *Geology and Mineral Wealth of the Sultanate of Oman*. M.P.M. Geological Documents. Ministry of Petroleum and Minerals, Directorate General of Minerals, Oman. 285 p.

Le Nindre, Y. M., Manivit, J., and Vaslet, D. (1987). *Histoire géologique de la bordure occidentale de*

la plate-forme arabe du Paléozoïque inférieur au Jurassique supérieur (en 4 livres). PhD thesis, University of P. et Marie Curie, Paris VI. 3 juin 1987.

Le Nindre, Y.-M., Manivit, J., and Vaslet, D. (1990a). Géodynamique et Paléogéographie de la Plateforme Arabe du Permien au Jurassique. In *Histoire Géologique de la Bordure Occidentale de la Plate-Forme Arabe, Volume 2*, Documents du BRGM no. 192. Editions du BRGM, Orléans. 273 p., 54 fig., 4 tabl., 4 annexes. ISSN 0211-2536, ISBN 2-7159-0947-5.

Le Nindre, Y. M., Manivit, J., and Vaslet, D. (1990b). Le Permo-Trias d'Arabie centrale. In *Histoire géologique de la bordure occidentale de la plate-forme arabe, Vol. 3*, Documents du BRGM n° 193. Editions du BRGM, Orléans. ISSN: 0221-2536, ISBN: 2-7159-0507-6, 290 p, 51 fig., 4 tabl., 11 pl., 3 annexes.

Le Nindre, Y. M., Vaslet, D., Énay, R., Manivit, J., and Al-Husseini, M. I. (2022). Sequence architecture of the Toarcian Marrat Formation: The Khashm adh Dhibi reference section. ResearchGate, 35 p.

Le Nindre, Y. M., Vaslet, D., Le Métour, J., Bertrand, J., and Halawani, M. (2003). Subsidence modelling of the Arabian platform from Permian to Paleogene outcrops. *Sediment. Geol.*, 156(1–4), 263–285.

Le Nindre, Y. M., Vaslet, D., and Manivit, J. (1983). Sedimentary evolution of Saudi Arabian Jurassic (Toarcian–Upper Oxfordian) deposits in outcrop between latitudes 24° N and 22° N. BRGM Open File Report BRGM-OF-03-05. 34 p, 3 fig., 4 tables, 7 appendixes. Ministry of Petroleum and Mineral Resources. Deputy Ministry for Mineral Resources. Jiddah, Kingdom of Saudi Arabia. 1403 A.H., 1983 A.D.

Le Nindre, Y. M., Vaslet, D., Vrielynck, B., Krystyn, L., Manivit, J., Memesh, A., Abdullah, M. S., and Davies, R. B. (2023). The Middle to Late Triassic of Central Saudi Arabia with emphasis on the Jilh Formation. Part I: lithostratigraphy, facies and paleoenvironment, palaeontology and biostratigraphic age calibration from outcrop studies. *C. R. Géosci.*, 355(S2), 1–31. (in this issue). Volume Spécial, Hommage à Jean Dercourt.

Lucic, D., Ivkovic, Z., Takec, D., Bubnic, J., and Koch, G. (2010). Depositional sequences and palynology of Triassic carbonate-evaporite platform deposits in the Palmyrides, Syria. In van Buchem, F. S. P., Gerdes, K. D., and Esteban, M., editors, *Mesozoic*

and Cenozoic Carbonate Systems of the Mediterranean and the Middle East: Stratigraphic and Diagenetic Reference Models, Geological Society, London, Special Publications, 329, pages 43–63. Geological Society of London.

Lunn, G. A. (2020). Dating and correlation of the Baluti Formation, Kurdistan, Iraq: Implications for the regional recognition of a Carnian "Marker Dolomite", and a review of the Triassic to Early Jurassic sequence stratigraphy of the Arabian Plate by G. A. Lunn G. A., S. Miller, and A. Samarrai. Reply to discussion by R. B. Davies and M. D. Simmons. *J. Pet. Geol.*, 43(1), 109–126.

Lunn, G. A., Miller, S., and Samarrai, A. (2019). Dating and correlation of the Baluti Formation, Kurdistan, Iraq: implications for the regional recognition of a Carnian "marker dolomite" and a review of the Triassic to Early Jurassic sequence stratigraphy of the Arabian Plate. *J. Pet. Geol.*, 42(I), 5–36.

Manivit, J., Le Nindre, Y. M., and Vaslet, D. (1990). Le Jurassique d'Arabie Centrale. In *Histoire Géologique de la Bordure Occidentale de la Plate-forme Arabe, Volume 4*, Document du BRGM n° 194. Editions du BRGM, Orléans. 559 p, 74 fig., 1 tabl., 12 pl. photo, 3 ann. (ann. 1: 12 pl.). ISSN: 0221-2536, ISBN: 2-7159-0508-4.

Manivit, J., Pellaton, C., Vaslet, D., Le Nindre, Y. M., Brosse, J. M., Breton, J. P., and Fourniguet, J. (1985a). *Geologic map of the Darma' quadrangle, Kingdom of Saudi Arabia. Geoscience map GM-101C, scale 1:250,000, sheet 24H*. Deputy Ministry for Mineral Resources, Ministry of Petroleum and Mineral Resources, Kingdom of Saudi Arabia. Explanatory notes, 33 p.

Manivit, J., Pellaton, C., Vaslet, D., Le Nindre, Y. M., Brosse, J. M., and Fourniguet, J. (1985b). *Geologic map of the Wadi Al Mulayh quadrangle, Kingdom of Saudi Arabia. Geoscience Map GM-92C, scale 1:250,000, sheet 22H*. Deputy Ministry for Mineral Resources, Ministry of Petroleum and Mineral Resources, Kingdom of Saudi Arabia. Explanatory notes, 32 p.

Manivit, J., Vaslet, D., Berthiaux, A., Le Strat, P., and Fourniguet, J. (1986). *Geologic map of the Buraydah quadrangle, Kingdom of Saudi Arabia. Geoscience Map GM-114 C, scale 1:250,000, sheet 26G*. Deputy Ministry for Mineral Resources, Ministry of Petroleum and Mineral Resources, Kingdom of Saudi Arabia. Explanatory notes, 32 p.

Maurer, F., Krystyn, L., Martini, R., Mcroberts, C., Rettori, R., and Hofmann, P. (2015). Towards a refined Arabian Plate Triassic stratigraphy: insights from the Musandam Peninsula (UAE & Oman). In *5th Arabian Plate Geology Workshop, Lower Triassic to Middle Jurassic Evaporite–Carbonate–Siliciclastic Systems of the Arabian Plate (Sudair to Dhruma and Time Equivalent), 8–11 February 2015, Kuwait.*

Maurer, F., Rettori, R., and Martini, R. (2008). Triassic stratigraphy, facies and evolution of the Arabian shelf in the northern United Arab Emirates. *Int. J. Earth Sci. (Geol. Rundsch.)*, 97, 765–784. First online: 22 May 2007.

Murris, R. J. (1981). Middle East: stratigraphic evolution and oil habitat. *Geol. Mijnbouw*, 60, 467–486.

Nicoll, R. S. and Foster, C. B. (1994). Late Triassic conodont and palynomorph biostratigraphy and conodont thermal maturation, North West Shelf, Australia. *AGSO J. Australian Geol. Geophys.*, 15(1), 101–118.

Nicoll, R. S. and Foster, C. B. (1998). Revised conodont-palynomorph biostratigraphic zonation and the stratigraphy of the Triassic of the western and northwestern margins of Australia and Timor. In Purcell, P. G. and Purcell, R. R., editors, *Sedimentary basins of Western Australia 2: Proceedings of Petroleum Exploration Society Australia Symposium, Perth, 1998*, pages 129–139.

Obermaier, M., Aigner, T., and Forke, H. C. (2012). Facies, sequence stratigraphy and reservoir/seal potential of a Jilh Formation outcrop equivalent (Wadi Sahtan, Triassic, Upper Mahil Member, Sultanate of Oman). *GeoArabia*, 17(3), 85–128.

Ogg, J. G. (2012). The triassic period. In Gradstein, F. M., Ogg, J. G., Schmitz, M., and Ogg, G., editors, *The Geological Time Scale*, pages 681–730. Elsevier, Amsterdam. Chapter 25.

Ogg, J. G. (2015). The mysterious Mid-Carnian "Wet Intermezzo" global event. *J. Earth Sci.*, 26(2), 181–191.

Ogg, J. G. and Chen, Z. Q. (2020). Chapter 25—The triassic period. In Gradstein, F. M., Ogg, J. G., Schmitz, M. D., and Ogg, G. M., editors, *The Geologic Time Scale 2020*, volume 2, pages 903–953. Elsevier, Amsterdam.

Pavia, G. and Martire, L. (2015). Indirect biostratigraphy in condensed successions: a case history from the Bajocian of Normandy (NW France). *Volumina Jurassica*, VII, 67–76.

Powers, R. W. (1968). *Lexique Stratigraphique International. Volume III, Asie, Fas. 10 b1, Arabia Saoudite.* Centre National de la Recherche Scientifique, Paris.

Powers, R. W., Ramirez, L. F., Redmond, C. D., and Elberg Jr., E. L. (1966). Geology of the Arabian Peninsula: Sedimentary geology of Saudi Arabia. United States Geological Survey Professional Paper 560-D, 147 p. 10 plates. US Department of Interior.

Ricou, L. E., Dercourt, J., Geyssant, J., Grandjacquet, C., Lepvrier, C., and Biju-Duval, B. (1986). Geological constraints on the Alpine evolution of the Mediterranean Tethys. *Tectonophysics*, 123, 83–122.

Ricou, L. E., Zonenshain, L. P., Dercourt, J., Kazmin, V. G., Le Pichon, X., Knipper, A. L., Grandjacquet, C., Sborshchikov, I. M., Lepvrier, C., Pechersky, D. M., Boulin, J., Sibuet, J. C., Savostin, L. A., Sorokhtin, O., Westphal, M., Lauer, J. P., and Biju-Duval, B. (1985). Méthodes pour l'établissement de neuf cartes paléogéographiques au 1:20 million s'étendant de l'Atlantique au Pamir pour la période du Lias à l'Actuel. *Bull. Soci. Géol. France*, I(5), 625–635.

Sadooni, F. N. and Alsharhan, A. S. (2004). Stratigraphy, lithofacies, and petroleum potential of the Triassic strata of the northern Arabian plate. *Am. Assoc. Pet. Geol. Bull.*, 88(4), 515–538.

Scotese, C. R. (2001). *Atlas of Earth History, Volume 1. Paleogeography.* PALEOMAP Project, Arlington, Texas.

Sharief, F. A. M. (1977). *Sedimentary facies of the Jilh Formation, Saudi Arabia. A regional paleostratigraphy and tectonic evolution of the Middle East during the Middle Triassic period.* PhD thesis, Rice University, Houston, Texas. 117 p.

Sharief, F. A. M. (1986). Depositional environments of the Triassic system in central Saudi Arabia. *Geol. J.*, 21, 403–420.

Sharland, P. R., Archer, R., Casey, D. M., Davies, R. B., Hall, S. H., Heward, A. P., Horbury, A. D., and Simmons, M. D. (2001). *Arabian Plate Sequence Stratigraphy.* GeoArabia Special Publication 2. Gulf PetroLink, Bahrain.

Sharland, P. R., Casey, D. M., Davies, R. B., Simmons, M. D., and Sutcliffe, O. E. (2004). Arabian plate sequence stratigraphy. *GeoArabia*, 9(1), 199–214.

Sodagar, T. M. (2015). Revelation of the Triassic Gas

Potential with Insight of Iso Frequency SpectralDe-composition in Saudi Arabia's Offshore. In *Proceedings of the SPE Middle East Oil & Gas Show and Conference, 8–11 March 2015, Manama, Bahrain*, SPE Paper 172625. 16 p.

Somma, R., Martín-Rojas, I., Estévez, A., Perrone, V., Zamparelli, V., and Delgado, F. (2008). The Ladinian to Carnian rifting stage recorded by the peritidal carbonate platform of the Betic Cordillera. In *STT-02 Structure and Formation of Rift Basins and Passive Margins from Surface to Depth: Observations and Modelling, International Geological Congress, Oslo 6–14th 2008*. Abstract.

Stewart, S. A., Reid, C. T., Hooker, N. P., and Kharouf, O. W. (2016). Mesozoic siliciclastic reservoirs and petroleum system in the Rub' Al-Khali basin, Saudi Arabia. *AAPG Bull.*, 100(5), 819–841.

Szabo, F. and Kheradpir, A. (1978). Permian and Triassic stratigraphy, Zagros Basin, southwest Iran. *J. Pet. Geol.*, 1, 57–82.

Taher, A., Al-Shateri, A., Al-Mehsin, K., Witte, J., Al-Zaabi, M., and Obaid, K. (2012). Tight gas exploration potential of Middle Triassic to Early Jurassiv successions in Abu Dhabi. In *Abu Dhabi Intarenational Petroleum Exhibition and Conference, Abu Dhabi, UAE, 11–14 November 2012*, Society of Petroleum Engineers, SPE-162355. 16 p, 20 figures, 1 table.

Tollmann, A. (1984). Entstehung und früher Werdegang de Tethys mit besonderer Berücksichtigung des mediterranen Raumes. *Mitt. Oesterreiscicher Geologischen Ges.*, 77, 93–113.

Tollmann, A. and Kristan-Tollmann, E. (1985). Paleogeography of the European Tethys from Palaeozoic to Mesozoic, and in the Triassic relations of the eastern part of the Tethys and Pa, thalassa. In Nakazawa, K. and Dickins, J. M., editors, *The Tethys: Her Paleogeography and Paleobiogeography from Palaeozoic to Mesozoic*, pages 3–22. Tokai University Press, Tokyo.

Urban, I., Demangel, I., Krystyn, L., Calner, M., Kovács, Z., Gradwohl, G., Lernpeiss, S., Maurer, F., and Richoz, S. (2023). Mid-Norian to Hettangian record and time-specific oolites during the end-Triassic Mass Extinction at Wadi Milaha, Musandam Peninsula, United Arab Emirates. *J. Asian Earth Sci. X*, 9, article no. 100138.

Vachard, D., Gaillot, J., Vaslet, D., and Le Nindre, Y. M. (2005). Foraminifers and algae from the Khuff

Formation (late Middle Permian-Early Triassic) of central Saudi Arabia. *GeoArabia*, 10(4), 137–186.

van Bellen, R. C., Dunnington, H. V., Wetzel, R., and Morton, D. M. (1959–2005). Lexique Stratigraphique International. 03 10 Asie, (Iraq), 333 pages. Reprinted by permission of CNRS by Gulf PetroLink, Bahrain.

Vaslet, D., Beurrier, M., Villey, M., Manivit, J., Le Strat, P., Le Nindre, Y. M., Berthiaux, A., Brosse, J. M., and Fourniguet, J. (1985). *Geologic map of the Al Faydah quadrangle, sheet 25G, Kingdom of Saudi Arabia, Geosciences Maps GM-102A, scale 1:250,000*. Saudi Arabian Deputy Ministry for Mineral Resources, Kingdom of Saudi Arabia. Explanatory notes, 28 p.

Vaslet, D., Le Nindre, Y. M., Vachard, D., Broutin, J., Crasquin-Soleau, S., Berthelin, M., Gaillot, J., Halawani, M., and Al-Husseini, M. I. (2005). The Permian-Triassic Khuff formation of central Saudi Arabia. *GeoArabia*, 10(4), 77–134.

Vaslet, D., Manivit, J., Le Nindre, Y.-M., Brosse, J.-M., Fourniguet, J., and Delfour, J. (1983). *Geologic map of the Wadi Ar Rayn quadrangle, Kingdom of Saudi Arabia. Geoscience Map GM-63C, scale 1:250,000, sheet 23H*. Deputy Ministry for Mineral Resources, Ministry of Petroleum and Mineral Resources, Kingdom of Saudi Arabia. Explanatory notes, 46 p.

Vickers-Rich, P., Rich, T. H., Rieppel, O., Thulborn, R. A., and Mcclure, H. A. (1999). A Middle Triassic vertebrate fauna from the Jilh Formation, Saudi Arabia. *Neues Jahrb. Geol. Paläontol. Abh.*, 213, 201–232.

Vrielynck, B. (1980). Précisions sur la stratigraphie du Trias d'Argolide (Péloponèse, Grèce), et consequences structurales. *Bull. Soc. Géol. France (7)*, XXII(3), 345–352.

Vrielynck, B. (1987). *Conodontes du Trias périméditerranéen : Systématique, stratigraphie*. PhD thesis, Université Claude-Bernard, France. Book, 300 p.

Vrielynck, B. and Cros, P. (1992). Les conodontes du Ladinien des faciès de transition bassin/plateforme dans les Dolomites (Latemar, Italie). Evolution sédimentaire et tectonique d'un massif caractéristique de la marge sud-téthysienne. *C. R. Acad. Sci., Paris*, II, 1223–1229.

Vrielynck, B., Dercourt, J., and Cottereau, N. (1994). Des seuils lithosphériques dans la Téthys. *C. R. Acad. Sci. Paris*, II, 1677–1685.

Zhou, S., Al-Hajhog, J., Simpson, M. A., Luo, M., Mohiuddin, M., and Tan, C. (2009). Study of Jilh formation. Overpressure and its prediction. In *Proceedings of the SPE/IADC Middle East Drilling Technol-* *ogy Conference and Exhibition, Manama, Bahrain 26–28 October 2009*, SPE Paper 125657. 17 p.

Ziegler, M. A. (2001). Late Permian to Holocene paleofacies evolution of the Arabian Plate and its hydrocarbon occurrences. *GeoArabia*, 6(3), 445–504.